Journal of Mammalian Evolution (2025) 32:48
https://doi.org/10.1007/s10914-025-09788-x

RESEARCH

Micromammal-based paleoprecipitation estimates for the late Middle and early Late Miocene record of the Vallès-Penedès Basin (Catalonia): Implications for primate habitats

Isaac Casanovas-Vilar[1] · Jan van Dam[1,2] · Chiara Angelone[1,3] · Marc Furió[1,4] · Israel García-Paredes[1,5] · Lars W. van den Hoek Ostende[6] · David M. Alba[1]

Received: 18 July 2025 / Accepted: 8 November 2025

Abstract

The densely sampled and well dated late Aragonian to Vallesian succession (late Middle to early Late Miocene, 12.5–9.0 Ma) of the Vallès-Penedès Basin (VP) in Catalonia has yielded one of the richest primate records in Eurasia, including hominoids and pliopithecoids. Here we present high-resolution mean annual precipitation (MAP) estimates derived from the ecological structure of small mammal assemblages to infer the paleoclimate and habitats associated with these primates. Our approach uses the relative abundance of arboreal and insectivore taxa as a paleoprecipitation proxy, producing robust results when sampling is sufficient. MAP values generally cluster around ~1,000 mm with low seasonality. Combined with mean annual temperature (~17–18 °C), this suggests a transitional climate between humid subtropical and Mediterranean regimes. These conditions would have supported diverse environments—subtropical evergreen broadleaf and mixed mesophytic forests interspersed with drier woodlands—consistent with the arboreal locomotor adaptations and inferred dietary preferences of VP primates. We find no evidence for distinct habitat partitioning between hominoids and pliopithecoids, nor for significantly more humid environments during primate-bearing intervals. Climatic parameters remained relatively stable even through major faunal turnovers such as the Vallesian Crisis (~9.7 Ma), indicating that local extinction of hominoids and other taxa was likely not driven by abrupt climate change, but rather by longer-term climatic deterioration or subtle environmental perturbations that affected the marginal habitats to which these species may have been restricted.

Keywords Climate · Mammals · Miocene · Paleoprecipitation · Seasonality · Spain

✉ Isaac Casanovas-Vilar
isaac.casanovas@icp.cat

[1] Institut Català de Paleontologia Miquel Crusafont (ICP-CERCA), Universitat Autònoma de Barcelona, Edifici ICTA-ICP, c/Columnes s/n, 08193 Cerdanyola del Vallès, Barcelona, Spain

[2] Department of Earth Sciences, Utrecht University, Vening Meinesz Building A, Princetonlaan 8a, Utrecht 3584 CB, the Netherlands

[3] Dipartimento di Scienze, Università degli Studi Roma Tre, Largo S. Leonardo Murialdo 1, Roma 00146, Italy

[4] Serra Húnter Fellow, Departament de Geologia, Universitat Autònoma de Barcelona, 08193 Cerdanyola del Vallès, Barcelona, Spain

[5] Departamento de Educación, Métodos de Investigación y Evaluación, Facultad de Ciencias Humanas y Sociales, Universidad Pontificia Comillas, c/Universidad Comillas 3-5, Madrid 28049, Spain

[6] Naturalis Biodiversity Center, P.O. Box 9517, Leiden 2300 RA, The Netherlands

Published online: 29 January 2026

Introduction

The study of long and continuous fossil records provides valuable insights into ecological and evolutionary processes that may not be apparent in modern ecosystems. For such records to be informative, they must be rich throughout their duration, and the fossils must be systematically studied to ensure robust taxonomic data. Additionally, accurate dating is critical for understanding patterns occurring at the scale of thousands of years. A prime example of such a record is the Miocene terrestrial vertebrate fossils from the Siwaliks of Pakistan (Barry et al. 2002; Flynn et al. 2016; Badgley et al. 2025), but various Iberian regions, like the Calatayud-Montalbán and Teruel basins (North Central Spain; Van der Meulen et al. 2012; García-Paredes et al. 2016; Van Dam et al., 2001, 2023) or the Vallès-Penedès Basin (VP; Catalonia, Spain; Casanovas-Vilar et al. 2016b, 2022b), have a comparable quality. The VP has yielded a rich fossil record of terrestrial vertebrates ranging from the Early to the Late Miocene (~20–7 Ma; Casanovas-Vilar et al. 2016b, 2022b). Thanks to detailed bio- and magnetostratigraphic control (Garcés et al. 1996; Agustí et al. 1997; Casanovas-Vilar et al. 2016b; Alba et al. 2017, 2019, 2022a), the record from this basin is amenable to analyses of paleobiodiversity dynamics and paleoenvironmental changes through time—particularly, for high-resolution intervals (Casanovas-Vilar et al. 2022b), such as the Miocene Climatic Optimum, the Middle/Late Miocene and Aragonian/Vallesian transitions (best represented at the Abocador de Can Mata (ACM) composite sequence; Alba et al. 2017, 2022a), and the Vallesian Crisis through the early/late Vallesian boundary (Casanovas-Vilar et al. 2014, and references therein). One of the advantages of the VP record relative to other densely sampled Miocene sequences from elsewhere (such as those from the Siwaliks; Barry et al. 2002; Flynn et al. 2016; Badgley et al. 2025) is the restricted size of the basin (100 km long by 12–14 km wide; Fig. 1). This reduces the potential influence of spatial differences (due to latitudinal climatic gradients as well as physiographic factors) when investigating the interplay between paleoenvironmental changes and paleobiodiversity dynamics through time.

Since Crusafont-Pairó's original definition of the Vallesian European land mammal age (ELMA) (Crusafont Pairó 1950; Crusafont Pairó and Truyols Santonja 1960), the dispersal of hipparionin equids and other eastern faunal elements has been recognized at its onset at 11.2 Ma (Garcés et al. 1996; see also Casanovas-Vilar et al. 2016b; Alba et al. 2022a). For a long time, it was thought that the dispersal of these faunal elements did not involve any significant faunal turnover, with the Aragonian/Vallesian boundary considered barely noticeable in VP small mammal assemblages (Agustí et al. 1985, 1997; Casanovas-Vilar et al. 2016a, b). In contrast, the early/late Vallesian boundary coincided with a more dramatic change, the so-called Vallesian Crisis at about 9.7 Ma (e.g., Agustí and Moyà-Solà 1990; Agustí et al. 1997, 1999). More recently, these views have been challenged, with suggestions that the Vallesian Crisis may be exaggerated due to sampling bias (Casanovas-Vilar et al. 2014), and that the Aragonian/Vallesian transition implied a more important turnover than initially thought (Alba et al. 2022a). These new interpretations are due to the improvements in the VP record quality over the past decades, which include revised ages of key sites (e.g., Alba et al. 2019, 2022a, 2024b) and continuous paleontological work at ACM, which has produced a dense and well-dated sequence from 12.6 to 11.1 Ma (Alba et al. 2006, 2017, 2022a; Moyà-Solà et al. 2009b; Casanovas-Vilar et al. 2022b).

Better understanding of the VP record has been shaped by various generations of Catalan paleontologists and geologists, starting with Miquel Crusafont-Pairó (Alba and Casanovas-Vilar 2022), whose foundational work during the 1940–1970s was continued by his successors at the institute he founded in 1969 in Sabadell (Truyols i Santonja 1986; Crusafont i Sabater 2019). Among them, Salvador Moyà-Solà made key contributions to the study of VP faunas (for a detailed review of his research trajectory, see Alba 2025). Initially collaborating with Jordi Agustí, who studied the rodent faunas in detail, his work on the bovid turnover in the area was instrumental for the proposal of the Vallesian Crisis (Agustí and Moyà-Solà 1990; Moyà-Solà and Agustí 1990). Later on, in collaboration with Meike Köhler he shifted his attention to primates and their renewed excavations at Can Llobateres not only led to major fossil hominoid finds (Moyà-Solà and Köhler 1993, 1996), but also stimulated parallel magnetostratigraphic correlations of the Vallesian in its type area (Agustí et al. 1996, 1997; Garcés et al. 1996). In the early 2000 s, his efforts to protect the fossiliferous area of els Hostalets de Pierola during the expansion of the Can Mata landfill (Alba 2025) enabled further spectacular primate discoveries (e.g., Moyà-Solà et al. 2004, 2009a, b; Alba et al. 2010c, 2015) and helped to consolidate the Catalan school of vertebrate paleontology and promote further research on primates (Alba 2025). In this regard, it is noteworthy that Moyà-Solà, despite the focus on fossil primates for more than three decades, never neglected the study of other taxa. He actively promoted fieldwork, and, even if not devoting himself specifically to paleoecological research, Moyà-Solà always emphasized the importance of other faunal elements to adequately infer the paleoenvironmental conditions in which fossil primates lived and, ultimately, evolved. This is best exemplified by a visit that Moyà-Solà's team paid to the team of paleoanthropologist David Pilbeam at Harvard University in 2013, in which it was agreed that, beyond taxonomic and phylogenetic discrepancies, it was

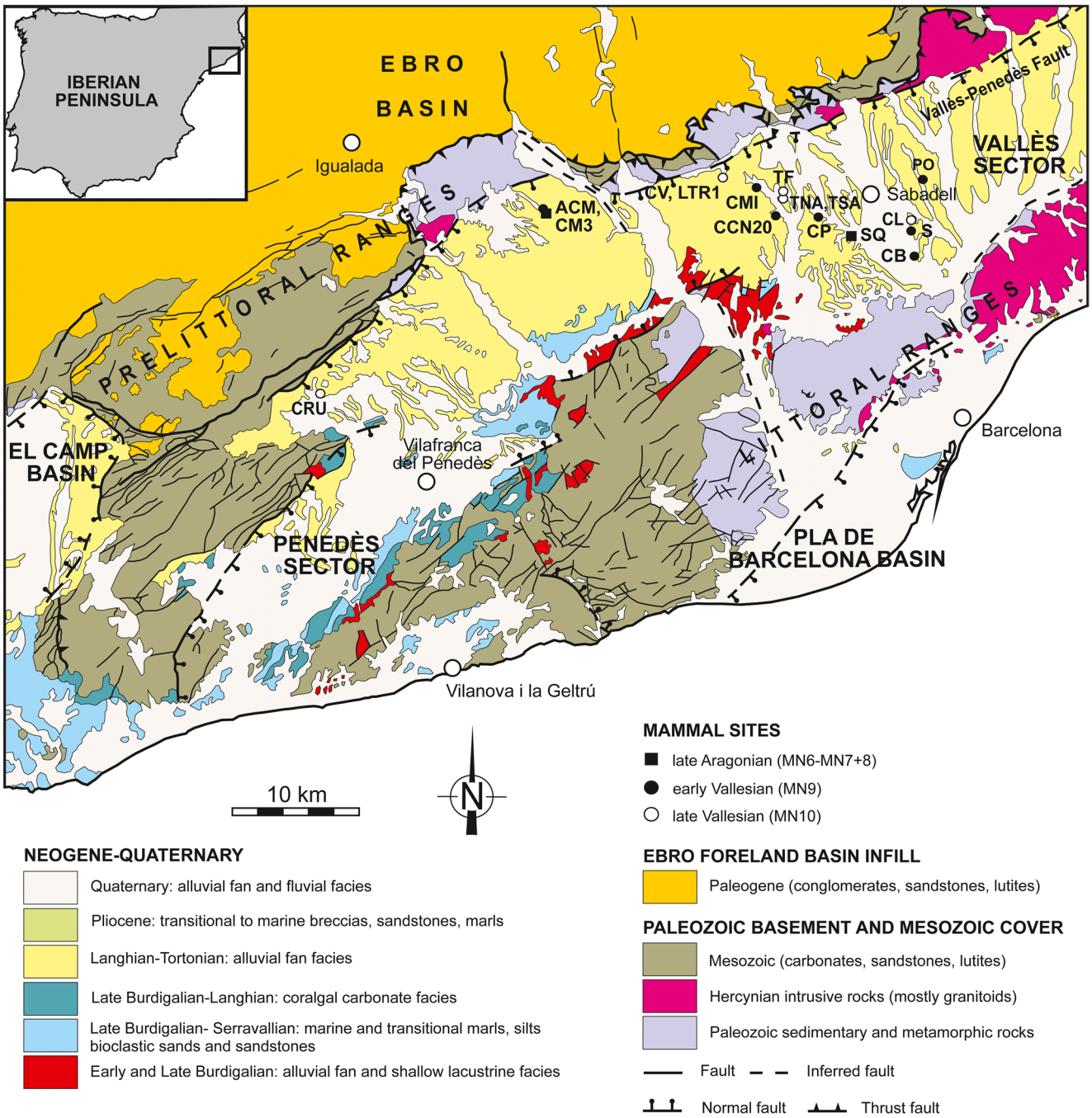

Fig. 1 Simplified geological map of the Vallès-Penedès Basin showing major vertebrate sites dated to 12.5–9.0 Ma (late Aragonian–Vallesian). Locality acronyms are as follows: ACM, Abocador de Can Mata (including Ecoparc de Can Mata; although the symbol used stands for the late Aragonian the series ranges from the late Aragonian to the early Vallesian); CB, Castell de Barberà; CCN20, Creu de Conill 20; CL, Can Llobateres; CM3, Can Mata 3; CMI, Can Missert; CP, Can Poncic; CRU, Can Cruset; CV, Ceràmiques Viladecavalls; LTR1, La Tarumba 1; PO, Polinyà; S, Santiga; SQ, Sant Quirze; TF, Torrent de les Febulines; TNA, Trinxera Nord Autopista; TSA, Trinxera Sud Autopista. Modified from Casanovas-Vilar et al. (2016b: fig. 1)

mandatory to investigate the paleoenvironmental and paleoecological context of Miocene apes to adequately understand their evolutionary history (Alba 2025). This visit was truly inspirational for two of the authors of this paper (I.C.V. and D.M.A.), who ever since then joined increased efforts to investigate the interplay between paleoenvironmental and paleobiodiversity dynamics based on the VP faunas.

The VP is not only renowned for its dense and continuous Miocene vertebrate record, but also because of the presence of both hominoid and pliopithecoid primates. The first

primate find from the basin dates back to the 1920s (Van der Made and Ribot 1999), and later significant contributions were made by Crusafont and coworkers from the 1940s onward (e.g., Villalta Comella and Crusafont Pairó 1941; see review in Alba 2012). However, primate research in the VP took a quantum leap under the leadership of Moyà-Solà (Alba 2025), and now the area is regarded as one of the best records of Miocene primates in Europe (Urciuoli and Alba 2023). Multiple primate-bearing localities are known, of which many are dated with 0.1 Ma accuracy (Table 1; see also Alba et al. 2022a; Urciuoli and Alba 2023). As for the associated paleoclimate and paleoenvironments, the

Table 1 Primate taxa by locality occurrences in the Vallès-Penedès Basin. For each locality, the site to which it belongs is indicated together with maximum (Max) and minimum (Min) age ranges. Age data compiled and updated from Alba et al. (2022a, 2025); Urciuoli and Alba (2023), references correspond to the main primary literature where the fossils were described

Species	Locality (site)	Max age	Min age	References
Anoiapithecus brevirostris	ACM/C1-E* (ACM)	12.4	12.3	Alba et al. (2013)
Pliopithecoidea indet.	ACM/C3-B2 (ACM)	12.1	12.1	Alba et al. (2012c)
Dryopithecus fontani	Can Mata s.l. (Hostalets)	12.0	11.0	Van der Made and Ribot (1999)
Pierolapithecus catalaunicus	ACM/BCV1 (ACM)	12.0	12.0	Moyà-Solà et al. (2004)
Anoiapithecus brevirostris	ACM/C3-Aj (ACM)	12.0	12.0	Moyà-Solà et al. (2009a); Alba et al. (2013)
Anoiapithecus brevirostris	ACM/C4-Cp (ACM)	12.0	12.0	Alba et al. (2024a)
'*Sivapithecus*' *occidentalis* species inquirenda	Can Vila (Hostalets Inferior)	12.0	12.0	Alba et al. (2020)
Dryopithecus fontani	ACM/C3-Ae (ACM)	11.9	11.9	Moyà-Solà et al. (2009b)
Dryopithecus fontani	ACM/C4-Ap (ACM)	11.9	11.9	Alba and Moyà-Solà (2012a)
cf. *Dryopithecus fontani*	ACM/C3-Az (ACM)	11.9	11.9	Moyà-Solà et al. (2009b)
'*Sivapithecus*' *occidentalis* species inquirenda	ACM/BCV4 (ACM)	11.9	11.9	Alba et al. (2020)
Pliopithecus canmatensis	ACM/C4-A1 (ACM)	11.7	11.7	Alba et al. (2010c)
Pliopithecus canmatensis	ACM/BCV5 (ACM)[a]	11.9	11.9	Alba et al. (2022a)
Pliopithecus canmatensis	ACM/C5-C3 (ACM)	11.9	11.9	Alba et al. (2010c)
Pliopithecus canmatensis	ACM/C5-C4 (ACM)[a]	11.8	11.8	Alba et al. (2022a)
Pliopithecus canmatensis	ACM/C4-Cb (ACM)	11.8	11.8	Alba et al. (2010c)
Pliopithecus canmatensis	ACM/C5-C2 (ACM)	11.8	11.8	Alba et al. (2010c)
Pliopithecus canmatensis	ACM/C5-A8 (ACM)	11.8	11.8	Alba et al. (2010c)
Dryopithecinae indet.	ACM/C8-Au (ACM)[a]	11.8	11.8	Alba et al. (2022a)
Dryopithecinae indet.	ACM/C8-B* (ACM)[a]	11.7	11.7	Alba et al. (2022a)
Dryopithecinae indet.	ACM/C5-D1 (ACM)[a]	11.6	11.6	Alba et al. (2022a)
Pliobates cataloniae	ACM/C5-D1 (ACM)	11.6	11.6	Bouchet et al. (2024)
Pliobates cataloniae	ACM/C8-A4 (ACM)	11.6	11.6	Alba et al. (2015), Bouchet et al. (2024)
Hispanopithecus sp.	Polinyà 2 (Polinyà)	11.2	9.7	Golpe Posse (1993)
Dryopithecinae indet.	Can Mata 1 (Hostalets)	11.6	11.2	Golpe Posse (1993)
Crouzeliinae indet.	Trinxera del Ferrocarril-Sant Quirze (Sant Quirze)	11.6	11.2	Harrison et al. (2002), Bouchet et al. (2025)
Crouzeliinae indet.	Can Feliu 2 (Sant Quirze)	11.2	11.2	Bouchet et al. (2025)
cf. *Dryopithecus fontani*	Castell de Barberà (Castell de Barberà)	11.2	11.2	Alba et al. (2011), Almécija et al. (2012)
Barberapithecus huerzeleri	Castell de Barberà (Castell de Barberà)	11.2	11.2	Alba and Moyà-Solà (2012b)
Hispanopithecus crusafonti	Can Poncic 1 (Can Poncic)	10.3	10.0	Golpe-Posse (1993), Begun (1992)
Hispanopithecus sp.	EDAR13 (EDAR)[a]	10.3	10.0	Alba et al. (2018)
Hispanopithecus laietanus	Can Feu 1 (Can Feu)	10.0	9.7	Alba et al. (2012a)
Hispanopithecus cf. *laietanus*	Can Pallars i Llobateres-M (Can Pallars i Llobateres)	10.0	9.7	Alba et al. (2018)
Hispanopithecus laietanus	Can Llobateres 1 (Can Llobateres)	9.8	9.8	Golpe Posse (1993); Begun et al. (1990); Alba et al. (2012b)
Hispanopithecus laietanus	Can Llobateres 2 (Can Llobateres)	9.6	9.6	Moyà-Solà and Köhler (1993, 1996)
Hispanopithecus laietanus	La Tarumba 1 (La Tarumba)	9.6	9.6	Golpe Posse (1993)
Egarapithecus narcisoi	Torrent de les Febulines (Can Jofresa)	9.0	9.0	Moyà-Solà et al. (2001)

[a] Unpublished remains. In these cases, the references correspond to publications where the material was reported or identified

relatively few studies have mostly focused on selected ACM localities (e.g., Casanovas-Vilar et al. 2008; DeMiguel et al. 2021) and, most notably, in the well-known Can Llobateres site (e.g. Begun et al. 1990; Alba, 2012; Marmi et al. 2012; Arranz et al. 2023). However, synthetic studies on climate and primate habitat change throughout the VP record are still lacking.

Here we provide small-mammal based paleoprecipitation estimates for the VP from 12.5 to 9.0 Ma (late Aragonian–Vallesian), thus covering the entire range of Miocene primates in the basin (Table 1). This time span also represents the most densely sampled and well-dated part of the Miocene record of the VP, particularly for small mammals (Casanovas-Vilar et al. 2016a, b, 2022b), thus providing the required large sample size and time resolution for these analyses. Because arboreal and insectivorous small mammals show a strong relationship with precipitation, ecological structure of small mammal assemblages has been successfully used to infer Neogene paleoprecipitation patterns at regional (Van Dam et al. 2006, 2023) and continental (Van Dam 2006; Van Dam and Utescher 2016) scales. Here, we apply these methods to the VP record to reconstruct paleoprecipitation during the late Aragonian and Vallesian and combine these with temperature estimates to infer prevailing biomes and primate habitats.

Geological background

The VP is a half-graben near the coastline bounded by the horst defined by the two parallel Catalan Coastal (Prelittoral and Littoral) Ranges (Fig. 1). The basin basement crops out at the surrounding reliefs and consists of Paleozoic metasediments intruded by plutonic rocks unconformably covered by Mesozoic and Paleogene sedimentary rocks. Until the Middle Miocene, the VP presented a typical graben profile but was effectively turned into a half-graben due to tectonic activity and subsidence concentrated at the Vallès-Penedès master fault at the northwest margin (Bartrina et al. 1992; Roca et al. 1999; Cabrera et al. 2004).

The formation of the VP was associated with a rifting process that affected much of western Europe and resulted from the collision of the African and Eurasian plates during the Late Oligocene (Roca and Guimerà 1992; Roca et al. 1999). However, sedimentary infill of the VP did not start until the Early Miocene (Ramblian ELMA) and spanned until the Late Miocene (Turolian ELMA; Casanovas-Vilar et al. 2016b, 2022b). Major features of the stratigraphic record of the VP were controlled by tectonic activity of its main bounding faults and by eustatic changes in the western Mediterranean (Cabrera et al. 1991, 2004; Cabrera and Calvet 1996). Most Early Miocene (Ramblian–early Aragonian) deposits correspond to alluvial fans sourced from the surrounding horsts, and occasionally small shallow lacustrine systems developed in the southeastern part of the basin (Cabrera Pérez 1979; Cabrera et al. 1991; Casanovas-Vilar et al. 2016b, 2021, 2022b). The Early to early Middle Miocene terrestrial vertebrate record is poorer than that of younger intervals, yet several sites are known, and recent field campaigns have resulted in the discovery of many new localities and a refining of their chronology (Casanovas-Vilar et al. 2016b, 2021, 2022a, b; Jovells-Vaqué and Casanovas-Vilar 2021).

The best and more densely sampled part of the VP record covers the late Middle Miocene and the beginning of the Late Miocene, thus corresponding to the late Aragonian and Vallesian ELMAs, roughly 12.5–9 Ma. Indeed, the VP is the type area of the Vallesian age (Crusafont Pairó 1950; Crusafont Pairó and Truyols Santonja 1960; Agustí et al. 1997), currently known to range from 11.2 to 8.9 Ma (Garcés et al. 1996; Van Dam et al. 2001; Dam et al. 2014; Hilgen et al. 2012; Casanovas-Vilar et al. 2016a; Alba et al. 2022a). At this time, basin subsidence and sedimentation was concentrated in the northwestern margin of the basin, resulting in the development of important alluvial fan systems sourced from the northwestern reliefs (Cabrera and Calvet 1996; Agustí et al. 1997; Casanovas-Vilar et al. 2016b, 2022b). Some alluvial fan systems (Fig. 1; Garcés Crespo 1995; Casanovas-Vilar et al. 2008) attained a radius of 10–15 km and may have even prograded over the southeastern margin reliefs. The mudstone-dominated medial to distal facies of these alluvial fan systems have yielded most of the vertebrate-bearing sites (Fig. 1), which concentrate in the area of els Hostalets de Pierola in the Penedès Sector of the basin, as well as around the cities of Sabadell, Terrassa, and Sant Quirze del Vallès in the Vallès Sector. Currently more than 950 late Aragonian to Vallesian localities are known from this area (data from the "Vallès-Penedès Miocene Vertebrates Paleobiodiversity Database", 14th May 2025, see below). Furthermore, thanks to detailed bio- and magnetostratigraphic control (Garcés et al. 1996; Agustí et al. 1997; Moyà-Solà et al. 2009b; Casanovas-Vilar et al. 2016a; Alba et al. 2017, 2019, 2022a), this part of the record has a great dating accuracy, up to the scale of 0.1 Ma, which is a prerequisite for high-resolution analyses such as the ones proposed in this work.

The uppermost part of the Miocene VP record is not well known, even though there are a few Turolian sites, including the rich macrovertebrate localities of Piera (~7.4–6.8 Ma; Casanovas-Vilar et al. 2016b). Before the end of the Miocene, tectonic subsidence stopped at the northwestern margin and the basin became completely filled up with sediments (Bartrina et al. 1992; Roca et al. 1999; Cabrera et al. 2004).

Materials and methods

Raw taxonomic data and generation of taxon counts per time bin

Data used for this paper are compiled in the "Vallès-Penedès Miocene Vertebrates Paleobiodiversity Database" (VPDB), a customized database used to record specimen and locality information for the VP (Casanovas-Vilar et al. 2018; Alba et al. 2022b). The VPDB is coordinated by D.M.A. and the copyright of the database and its management system is owned by the Institut Català de Paleontologia Miquel Crusafont (ICP). Currently, it is associated with various research projects led by ICP researchers and it is for internal use only by some ICP researchers and collaborators, as it includes both published and unpublished data. The database records both specimen-level and locality-level information and was specially devised to carry out diversity and turnover calculations, thus being simultaneously a collection and a research database (sensu Uhen et al. 2013). Specimen records are identified by their museum catalog number, referring mostly (but not exclusively) to specimens housed in the ICP. As for May 14th, 2025, the VPDB features 88,120 records and 1,789 localities. Vallès-Penedès Miocene small mammal data began to be compiled and reviewed in 2013, before the VPDB was created, to perform paleobiodiversity analyses (see Casanovas-Vilar et al. 2014). These data were uploaded to the VPDB and further expanded with the addition of new specimens and localities, yet the data used in this paper are still (and will always be) a work in progress from both a taxonomic and chronological point of view. Only a small part of the VP material has been published and described, particularly for well-known localities and taxonomical groups. However, when compiling the VPDB we ensured that the specimen data are uniform and reliable, so the VPDB data are more complete and consistent than those that can be retrieved from online databases, which generally record taxon by locality occurrences from literature.

The VPDB has multiple functionalities for searching data and calculating diversity metrics. In particular, it can be used to compute specimen counts per taxon for selected localities or equal-duration time bins (0.5 or 0.1 Myr). In this work, we used 0.1 Myr time bins rather than localities. Specimens are attributed to a given bin according to their provenance (site, locality and, when applicable, stratigraphic position). Specimens are assigned to bins according to their estimated ages, derived either from magnetostratigraphic data (see Casanovas-Vilar et al. 2014) when available, or otherwise from local biozonations (which typically span < 0.3 Myr; Casanovas-Vilar et al. 2016a). Bin attribution is automatically computed using a built-in algorithm (Alba et al. 2022b). Assignment is univocal when a specimen or locality has a single interpolated age or when its age uncertainty does not cross any of the bin boundaries. If the uncertainty does cross one or more boundaries, assignment becomes equivocal. In such cases, the algorithm applies a pseudo-random procedure to assign an age within the range defined by the youngest and oldest possible ages for that specimen or locality. However, if age uncertainty is more than three times bin duration, the algorithm refrains from providing an age. By convention, bin definition is forced so that the bottom boundary belongs to the preceding bin. For example, at the 0.1 Myr bin resolution, the 9.5–9.4 bin includes specimens dated between 9.49 and 9.40 Ma, so that a specimen or locality dated to 9.50 Ma would be assigned to the preceding bin (9.6–9.5 Ma).

Raw taxonomic data used for paleoprecipitation calculations were downloaded from the VPDB on May the 5th 2025. Species occurrences for 0.1 Myr bin were used for the interval from 12.5 to 9.0 Ma (data given in Online Resource 1). The fossils of these species were recovered from VP localities that correspond to medial and distal facies of alluvial fans, so that similar taphonomical conditions (or biases) can be assumed for the whole studied interval. However, some sites such as Can Llobateres and Castell de Barberà correspond to locally humid environments (wetlands). A total of 129 different taxa are included in the calculations. Taxonomic attributions modified by 'cf.' are assumed to belong to the specified taxon. For example, *Cricetulodon* cf. *sabadellensis* is assigned to *C. sabadellensis* rather than counted as a distinct species. In contrast, attributions modified by 'aff.' are counted as distinct species, since the modifier implies that the taxon most likely belongs to a different (probably new) species. For example, *Democricetodon* aff. *nemoralis*, occurring at Abocador de Can Mata ACM/C4-A1 site, likely represents a distinct species rather than *D. nemoralis*, which occurs in younger VP sites such as Castell de Barberà. Finally, identifications at higher taxonomic ranks than species are counted as a distinct species if the corresponding lower taxon is absent from the same bin. For example, *Desmanella* sp. and Myominini indet. are counted as species in the 11.2–11.1 bin because no other *Desmanella* or Myominini species are recorded in this bin. This option is more realistic than the alternative, which would omit all indeterminate attributions above the species rank.

Micromammal-based paleoprecipitation estimates

Paleoprecipitation variables were estimated using the Climate-Diversity Approach (CDA) of Van Dam (2006) and Van Dam and Utescher (2016). This method considers the taxonomic composition of micromammal assemblages specifically focusing on Rodentia, Lagomorpha, and Eulipotyphla. Actively flying species (Chiroptera) are generally

underrepresented in the studied sites and are excluded from the analyses. CDA uses the proportion of species in given ecological categories, which are more robust than absolute number of species against differences in sampling effort (Van Dam 2006). Specifically, the proportion of arboreal (tree dwelling) and invertivorous (feeding on insects and other invertebrates) species over the total number of species are used. The presence and abundance of primary consumers with arboreal feeding habits and/or locomotion (e.g., flying and tree squirrels, arboreal dormice) depends on productivity and complexity of the vegetation, which in turn is largely dictated by precipitation (Kay and Madden 1997; Van Dam 2006). On the other hand, invertivores benefit from higher invertebrate availability in moist environments and are also physiologically constrained by aridity, as small-bodied species like shrews have high metabolic rates and are prone to water loss and overheating in dry conditions (Reumer 1995; Van Dam 2006). Assignment of species to the 'arboreal' or 'invertivorous' categories follows Van Dam (2006), as modified by Van Dam and Utescher (2016) and Van Dam et al. (2023). Semiaquatic taxa, which in our case only include beavers, are excluded from the calculations because their presence is linked to the occurrence of permanent water bodies, which may depend on other factors (e.g., topography, sedimentary environment) besides rainfall. A minimum sample size of 100 specimens per bin is taken as a cut-off criterion for the bin to be included in the calculations, as it is considered the minimum sample size to record a sufficiently large number of species (Van Dam 2006; Van Dam and Utescher 2016).

Because the calibration set essentially consists of modern sites, the CDA method essentially predicts rainfall at geologically instantaneous times. By applying temporal binning, we basically assume that fossil faunas remain stable across the time represented by bins, or, more specifically, that relative species numbers are not affected by potential successive intra-bin species appearances and disappearances (e.g., due to climatic oscillations). This assumption is even stronger for range-through (RT) calculations (see below), in which presence/absence patterns are interpolated across entire bins. Assuming no bias due to unrecorded faunal change, we followed Van Dam et al. (2023) criterion for the treatment of sites without frequency information so that only bins containing at least 10 species were included in the calculations. This approach allowed all bins to be incorporated into the RT calculations.

We estimate three rainfall variables: mean annual precipitation (MAP), precipitation in the driest month (LMP), and precipitation during the wettest month (HMP). Precipitation seasonality is represented by the difference between LMP and HMP. To calculate these parameters, first the percentage of arboreal (arboreality index, PA) and invertivorous (invertivory index, PI) micromammal species must be computed. We used the equations of Van Dam and Utescher (2016) to estimate MAP and HMP, whereas LMP was estimated with that of Van Dam et al. (2023):

$$MAP = 11.080 + 47.178\ \ln^2(PA+1) + 12.492\ PI \quad (1)$$

(R^2=0.82)

$$LMP = 1.689 + 10.801\ \ln(PA+1) \quad (2)$$

(R^2=0.79)

$$HMP = 8.108 + 1.674\ \ln^3(PA+1) + 1.896\ PI \quad (3)$$

(R^2=0.74)

These variables are estimated for each time bin and presented together with associated standard errors and 95% individual prediction intervals. Calculations were carried out using SPSS Statistics v. 29.0 software (IBM Corp. 2022).

Assessment of sample size biases

Previous studies of the VP small mammal record have shown that rodents and insectivores presumably adapted to humid forested environments are typically more rare than other species, showing a discontinuous record during the Vallesian and being only recovered when sample size is large enough (Casanovas-Vilar et al. 2014, 2016b). This has potentially important implications for our paleoprecipitation estimates, since the relative numbers of invertivorous and arboreal species are used to infer rainfall variables (see discussion in Van Dam and Utescher 2016). Therefore, these may potentially depend on sample size and yield too low values for small samples. Excluding the time bins with fewer than 100 small mammal specimens and considering relative proportions (PA, PI) rather than absolute numbers may partly solve this problem, but here we additionally evaluated the effects of sample size in the patterns of rare and common species in relation to PA and PI.

Firstly, we evaluated whether rare taxa predominantly correspond to invertivorous or arboreal species. To reduce the impact of sampling bias and the stochastic occurrence of rare taxa in large assemblages, we filtered the dataset by removing, within each bin, all species with relative abundances below 5%. This threshold ensures that only ecologically meaningful taxa contribute to inter-bin comparisons and follows common practice in paleoecological and ecological studies dealing with uneven sampling effort (e.g., McGarigal et al. 2000). It is, however, more

restrictive than in some other fields—such as Quaternary palynology—where only taxa below 1% are typically excluded (e.g., Chevalier et al. 2020). After filtering, we counted the number of species in each ecological category (arboreal, invertivorous, semiaquatic, and others) that remained. For each bin, filtered data were compared to original data using Fisher's exact test, which is more appropriate than the chi-squared test for small sample sizes, and evaluates whether the observed differences in proportions are likely due to chance (Hammer and Harper 2024). For bins where no invertivorous or arboreal taxa are recorded (either before or after filtering), the contingency table is incomplete, and the test cannot be run. In these cases, we recorded N/A for the *p*-value and used logical flags ('true' or 'false') to indicate which ecological group(s) were missing from the data.

Secondly, we also tested the correlation of PI, PA, MAP, HMP and LMP with sample size. Since the distribution of the data is obviously not normal, correlation was tested using the non-parametric Kendall's rank correlation, which is more robust than other non-parametric correlation methods (e.g., Spearman's rank-order correlation) for small samples ($n < 30$; Puth et al. 2015). These correlations were performed using both the raw calculations (only considering bins with sample size > 100 specimens) as well as the alternative ones using RT approach (see below). All calculations were performed using R version 4.5.0 (R Core Team 2025).

Range-through approach

Alternative calculations of rainfall variables were also computed using a standard RT approach to estimate species richness across successive time bins. This method assumes a taxon to be present in a given interval if it is recorded before and after it, even if it is not directly observed in that interval. As such, it mitigates the effects of incomplete sampling and preservation (Foote 2000) and is widely used in macroevolutionary and paleoecological studies (e.g., Barry et al. 2002; Casanovas-Vilar et al. 2005, 2010, 2014; Badgley and Finarelli 2013; Domingo et al. 2014; Badgley et al. 2025). Given the high-resolution chronological framework (0.1 Myr bins) and the dense sampling for the VP, this approach provides a conservative but informative estimate of taxonomic richness through time (RT data are given in Online Resource 2). However, RT may assume a range continuity which may not be real and consequently overestimate taxonomic richness for some intervals. Therefore, we provide RT calculations as a comparison and alternative to those based on raw data, further discussing differences and patterns that may most likely arise from variations in record quality.

Paleotemperature data and climate classification

Temperature is a climatic variable as important as (or even more important than) precipitation and is the basis for various climate classification schemes (e.g., Whittaker 1971; Walter 1979; Peel et al. 2007; Beck et al. 2023). Micromammal assemblages have also been previously used to estimate Miocene paleotemperatures. Various approaches have found a positive correlation between the number of cricetid and murid species and temperature (Legendre et al. 2005; Montuire et al. 2006), but these yielded unrealistically low estimates when the number of species is low (less than ~6–8). Unfortunately, independent paleotemperature proxies based on local macroflora, pollen records, or stable isotope data are not available for the studied area and interval. However, horse tooth $\delta^{18}O$-based annual temperatures for several sites in the Calatayud-Montalbán and Teruel Basin in the Spanish inland are in the order of 15–17 °C for the Vallesian (Van Dam and Reichart 2009). If latitudinal gradients were the same as today, temperatures ~3.5 °C higher would be expected for the VP. Because of the uncertainties associated and restriction to a few age points only, we applied an alternative method using the ocean surface paleotemperature equations of Hansen et al. (2013) based on deep-sea benthic foraminifera $\delta^{18}O$ to estimate surface temperature indirectly. We used the loess 10-point smoothed global $\delta^{18}O$ dataset from Westerhold et al. (2020; table S34) to calculate mean $\delta^{18}O$ values per time bin. Global mean deep-sea (T_{do}) and surface air temperatures (T_s) were then calculated using Hansen et al.'s (2013) equations (= equation (6) from Westerhold et al. 2020: table S7) for each time bin. Finally, the temperature anomaly relative to present-day conditions (Δt) was calculated by subtracting the 1961–1990 mean temperature (14.15 °C) from Ts for each bin (Westerhold et al. 2020, Eq. 7). This anomaly, usually 1.5–2 °C higher than present, was added to the mean annual temperature (MAT) of Barcelona (15.5 °C) between 1961 and 1990 (Servei Meteorològic de Catalunya 2008) to estimate paleotemperature for each time bin.

The primary goal of estimating paleotemperatures for the studied interval is to combine this information with paleoprecipitation estimates and infer the kind of climate present in the VP during the studied interval. To do so, we rely on the Köppen-Geiger climate classification, which remains as one of the most well-known and widely used climate classification systems to this day. It was developed in the late 19th century by Russian-German geographer and climatologist Wladimir Köppen and later refined by meteorologist Rudolf Geiger (Beck et al. 2023). This classification divides global terrestrial climates into five major classes and 30 subclasses based on threshold values and seasonality of monthly air temperature and precipitation (for updated maps, see Beck et

al. 2023). The Köppen-Geiger system categorizes climates into five main groups: A (tropical), B (arid), C (temperate), D (continental), and E (polar). A second letter denotes seasonal precipitation patterns, while the third letter indicates temperature characteristics. Here, we partly follow the Trewartha climate classification (Trewartha and Horn 1980) and refer to the hot-summer warm-temperate climates (Cfa, Cwa) as subtropical to clearly distinguish them from colder temperate ones. The Mediterranean climate (Csa) is also subtropical in this system, but here we refer specifically to it as Mediterranean. Considering the temperature range for the Miocene, we will focus our discussion on tropical, arid, and especially subtropical/temperate climates, leaving cold and polar ones out.

The defining criteria for Köppen-Geiger climate classes and subclasses (see Peel et al. 2007; Beck et al. 2023) are presented in Table 2. However, we must note that many criteria cannot be evaluated using our data, as these rely on the timing of the dry/wet season (summer or winter), temperatures during the coldest and warmest months or the number of months with temperatures above 10 °C. Therefore, we adapted the criteria of climate classification using more generally defined climatic variables (Table 2). Distinction between tropical (A), subtropical (Cxa) and temperate (Cxb or Cxc) climates prominently considers the temperature during the coldest or warmest months. Since only MAT can be estimated using our methods, we compiled typical MAT values using the data of the meteorological stations in Peel et al. (2007) and broadly defined MAT ranges for each climate class (Table 2). Tropical climates have MAT > 18 °C (and more typically over 24 °C), for subtropical and warm-temperate climates MAT ranges between 12 and 18 °C, being 16–18 °C for Cxa, 14–16 °C for Cxb, and 12–14 °C for the colder Cxc. Similarly, given that our methods cannot tell the season in which the driest (LMP) and wettest (HMP) months occurred, we used LMP as equivalent to the driest month of summer and/or winter and HMP as the equivalent to the wettest month of summer and/or winter to distinguish between Cs and Cw climates. Moreover, since precipitation differences between driest and wettest months are far greater in the monsoon-influenced Cw climates, both climates can be distinguished. Finally, arid (B) climates are defined according to a precipitation threshold ($P_{treshold}$; see Table 2) that can take three different values if more than 70% of MAP occurs in summer, winter or in another season, respectively. Since we cannot infer in which season precipitation fell, the three possible definitions of $P_{threshold}$ are considered simultaneously to identify arid climates. These modifications allow for the assignment of a particular Köppen-Geiger climate class for each time bin. However, given that we adapted the defining criteria, these assignments must be considered as working hypotheses only, which should be checked against other proxy data (e.g., palynology, macrofloral data) or modelling results.

Table 2 Simplified Köppen-Geiger classification of tropical, arid, and temperate climates and broad defining criteria. Since our calculations only allow estimating the mean annual temperature (MAT), mean annual precipitation (MAP), wettest month precipitation (HMP), and driest month precipitation (LMP) the same defining criteria (see Beck et al. 2023) cannot be used, and a modified version is also presented (see text for details). Tropical (A) and arid (B) climates are mostly excluded for the Iberian late Aragonian and Vallesian, so their subdivisions are not presented. Temperature and precipitation values are in °C and mm, respectively. Variable definitions: MAT = mean annual temperature; T_{cold} = air temperature of the coldest month; T_{hot} = air temperature of the warmest month; T_{mon10} = number of months with air temperature > 10 °C (unitless); MAP = mean annual precipitation; HMP = precipitation in the wettest month; LMP = precipitation in the driest month; P_{sdry} = precipitation in the driest month in summer; P_{wdry} = precipitation in the driest month in winter; P_{swet} = precipitation in the wettest month in summer; P_{wwet} = precipitation in the wettest month in winter; $P_{threshold} = 2 \times MAT$ if > 70% of precipitation falls in winter, $P_{threshold} = 2 \times MAT + 28$ if > 70% of precipitation falls in summer, otherwise $P_{threshold} = 2 \times MAT + 14$. Since our paleoprecitation estimates cannot infer if most of the precipitation fell in winter or summer, the three possible definitions of $P_{threshold}$ are considered simultaneously to identify arid (B) climates

Type	Subtype 1	Subtype 2	Description	Defining criteria	Criteria used here
A			Tropical	Not (B) $T_{cold} > 18$ °C	Not (B) & MAT > 18 °C
B			Arid	$MAP > 10 \times P_{treshold}$	$MAP > 10 \times P_{treshold}$
C			Temperate & subtropical	Not (B) & $T_{hot} > 10$ °C & $T_{cold} = 0$–18 °C	Not (B) & MAT = 12–18 °C
	s		-dry summer	$P_{sdry} < 40$ & $P_{sdry} < P_{wwet}/3$	LMP < 40 & LMP < HMP/3
	w		-dry winter	$P_{wdry} < P_{swet}/10$	LMP < HMP/10
	f		-without dry season	Not (Cs) or (Cw)	Not (Cs) or (Cw)
		A	-hot summer	$T_{hot} \geq 22$	MAT = 16–18 °C
		B	-warm summer	Not (a) & $T_{mon10} \geq 4$	MAT = 14–16 °C
		C	-cold summer	Not (a or b) & $1 \leq T_{mon10} < 4$	MAT = 12–14 °C

Abbreviations

Institutional abbreviations: ICP, Institut Català de Paleontologia Miquel Crusafont.

Fossil locality abbreviations: ACM, Abocador de Can Mata; **ACM/BCV1**, Barranc de Can Vila 1; **CLL**, Can Llobateres.

Climatic variable abbreviations: HMP, precipitation during the wettest month (in mm); **LMP**,precipitation during the driest month (in mm); **MAP**, mean annual precipitation (in mm), **MAT**, mean annual temperature (in °C).

Other abbreviations: CDA, climate diversity approach; **ELMA**, European land mammal ages (after Hilgen et al., 2012); **GPTS**, Geomagnetic Polarity Time Scale (after Ogg 2020); **MN**, European mammal Neogene units (after Mein 1975, 1999), age boundaries follow Hilgen et al. (2012), Van Dam et al. (2014) and Casanovas-Vilar et al., (2016a); **PA**, arboreality index; **PI**, invertivory index; **RT**, range-through; **VP**, Vallès-Penedès Basin; **VPDB**, Vallès-Penedès Miocene Vertebrates Paleobiodiversity Database.

Results

Sample size effects on paleoprecipitation proxies

Raw data reveal several gaps (Fig. 2e; Online Resource 3: Table S1), especially during the Vallesian, with no records between 10.9 and 10.8, 10.7–10.6, 10.5–10.4 and 9.3–9.2 Ma. For some Vallesian bins, the number of specimens is below 100, thus precluding calculations for the 11.0–10.6, 10.2–10.1, 9.9–9.8 and 9.7–9.3 Ma. The late Aragonian is more densely sampled and only shows two bins with less than 100 specimens, between 12.3 and 12.2 and 11.5–11.4 Ma. Mean sample size is usually below 1,000 specimens (~200 specimens being typical), but for particular intervals (11.8–11.6, 11.2–11.1, 9.8–9.7 Ma) exceeds 2,000–3,000 specimens (Fig. 2e; Online Resource 3: Table S1).

Mean number of recorded taxa per bin is around 20, with peaks of 35–45 taxa coinciding with the best-sampled bins (Fig. 2a, e; Online Resource 3: Table S1). This points to obvious sampling effects on the number of taxa, although such sampling bias is not so clear for the proportion of taxa in each ecological category (Fig. 2c; Online Resource 3: Table S1). For most bins, PI and PA are around 20–25% and 30–35%, respectively. Arboreal and invertivorous taxa are diverse but numerically rare in the VP micromammal faunas, in such a way that filtering out all species with relative abundances below 5% results in the disappearance of almost all these taxa (Online Resource 3: Table S2). Amongst arboreal taxa, only the scansorial/arboreal sciurid *Csakvaromys bredai* is relatively abundant for most bins, whereas the invertivorous galericine erinaceid *Parasorex socialis* and, to a lesser extent, the heterosoricid *Dinosorex grycivensis* are common, particularly during the late Aragonian. The remaining arboreal and invertivore taxa are rare or anecdotic, although the same applies to many other taxa not assigned to these groups. Indeed, generally only species of the genera used to define the VP local biozones (i.e., *Hispanomys*, *Democricetodon*, *Megacricetodon*, *Cricetulodon*, and *Rotundomys*; see Casanovas-Vilar et al. 2016a) are abundant in all sites and retained after filtering.

The relative proportion of arboreal and invertivorous species in raw and filtered data was compared using Fisher's exact test (Online Resource 3: Table S3). The test could not be run if no invertivorous or arboreal taxa were present before or after filtering. Invertivorous taxa are present in 16 of the 20 bins with $n > 100$ specimens and, after filtering, disappeared from 14 bins. Therefore 87.5% of their occurrences were removed. As for arboreal taxa, these occurred in 19 of 20 bins and remained in 14 bins, so that 73.7% of their occurrences were removed after filtering. In the few cases in which arboreal and/or invertivorous taxa were not completely removed by filtering, Fisher's exact test detected highly significant differences between raw and filtered data in two out of four cases. These results show that the occurrence of most arboreal and invertivorous small mammal taxa in VP is highly dependent on sampling effort. However, the same applies to several taxa in other ecological categories and, since CDA relies on relative richness numbers, the critical parameters PI and PA, used to estimate paleoprecipitation, may be robust against sample size variations. A Kendall's correlation test reveals positive and highly significant correlations between sample size and the number of recorded taxa, PA, MAP, HMP and LMP, but not for PI (Table 3). This owes to the common presence of at least some invertivorous taxa in the studied record, but it is not enough to compensate for the effect of arboreal ones and results in significant positive correlations between sample size and paleoprecipitation estimates. This is evident for the 11.4–11.3 and 10.6–10.5 bins, which show relatively small sample sizes (~200 specimens) and consequently depleted MAP, HMP, and LMP estimates as compared with other intervals (Fig. 3).

Considering these correlations with sample size, we computed species richness, PI, PA and paleoprecipitation estimates after applying a RT approach to the whole dataset (Online Resource 3: Table S4). Using this approach, 35–40 taxa are recorded for most bins, except from 9.7 Ma onward, when these are reduced to ~20 (Fig. 2b; Online Resource 3: Table S4). PI and PA remain stable at around 35% and 30%, respectively, not showing major variations within bins (Fig. 2 d; Online Resource 3: Table S4). Apparently, correlation with sample size (Fig. 2e) is removed,

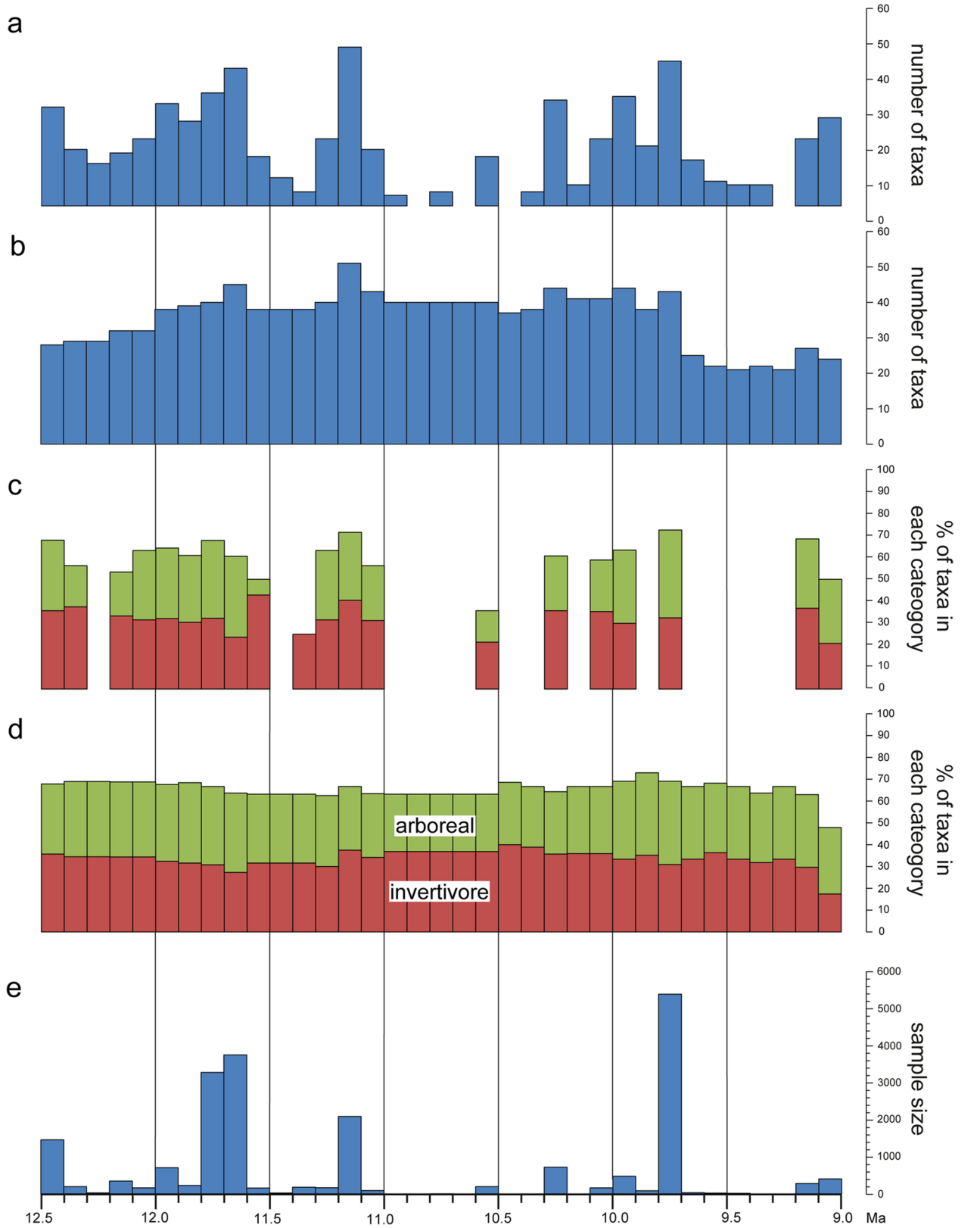

Fig. 2 Micromammal taxonomic richness (**a**–**b**), relative richness of ecological categories (**c**–**d**), and sample size (**e**, in number of identified cheek teeth) for each time bin. Results are presented for raw data (**a**, **c**) and after applying the range-through approach (**b**, **d**). For the calculation of the invertivorous and arboreal species percents, semi-aquatic species are excluded. For raw data, these percentages are not calculated for bins with sample size < 100 specimens. Data plotted in this figure are given in Online Resource 3: Tables S1 and S4

Table 3 Kendall's correlation test between sample size and total number of micromammal species, proportion of invertivorous (PI) and arboreal (PA) species, mean annual precipitation (MAP), precipitation during the wettest month (HMP) and precipitation during the driest month (LMP) for raw data and those using a range-through approach. For raw data, bins with sample size < 100 specimens are not included in the calculations. Significant results at $p < 0.05$ are indicated with asterisks

Variable	Raw data		Range-through approach	
	τ	*p*	τ	*p*
n taxa	0.663	5.94×10^{-5} *	0.210	0.073
PI	0.005	0.974	−0.360	0.003 *
PA	0.535	0.001 *	0.376	0.002 *
MAP	0.392	0.016 *	−0.029	0.808
HMP	0.423	0.009 *	0.115	0.340
LMP	0.535	0.001 *	0.376	0.002 *

yet Kendall's test still detects significant correlations between PI, PA, and sample size (Table 3). In addition, all paleoprecipitation estimates except LMP show no significant correlation with sample size. In conclusion, sampling effort may still affect our paleoprecipitation estimates, but applying the RT approach reduces some awkward variations between adjacent time bins that clearly result from uneven sampling (Fig. 3).

Micromammal-based paleoprecipitation estimates

MAP, HMP, and LMP estimates using raw and RT data are given in Tables 4, 5 and 6 and represented in Fig. 3. For each estimate, mean, standard error, and 95% confidence intervals are reported. MAP estimates based on raw and RT data differ, the latter being generally ~50–70 mm higher. However, estimated difference is more important for poorly-sampled bins (11.4–11.3 and 10.6–10.5 Ma), where it may be as much as ~400–600 mm, and it is negligible for the intervals with the largest sample size (11.8–11.6, 11.2–11.1, 9.8–9.7 Ma; Table 4). Mean annual precipitation, as estimated from RT data, shows little variations during the studied time interval, ranging between 789 and 1,082 mm, with values around 950–1,000 mm being more common (Table 4; Fig. 3). The maximum values correspond to the 9.9–9.8 Ma bin and the minimum ones to the 9.1–9.0 Ma bin (Table 4; Fig. 3), the very youngest interval. The occurrence of this minimum may reflect sample size and the lack of a suitable record after 9.0 Ma. Sample size for the 9.1–9.0 Ma bin is not particularly high (413 specimens; Online Resource 3: Table S4) and, given that there are no younger intervals to record the rare taxa, PI and PA might be underestimated resulting in somewhat lower paleoprecipitation estimates. The same may partly apply to the preceding 9.2–9.1 Ma bin, which also yields a low MAP estimate, but certainly does not apply to the latest Aragonian bins such as 11.7–11.6 Ma, for which estimated MAP is almost the same (970 mm; Table 4). Considering raw data and excluding the 11.4–11.3 and 10.6–10.5 Ma bins, MAP range is almost the same (754–1,083 mm). These poorly sampled bins yield low estimates of 323 and 630 mm, respectively, and resulted in abrupt paleoprecipitation declines as compared with adjacent intervals. After their exclusion, raw-data-based MAP estimates also show little variation throughout the studied interval. Maximum values correspond to the 11.2–11.1 Ma (1,083 mm) and the 9.8–9.7 Ma (1,068 mm) bins, thus approximately coinciding with the maxima estimated using RT data. After excluding the poorly sampled bins, MAP minima occur during the lower part of the record, in the 12.4–12.3 and 12.2–12.1 Ma bins, yielding values slightly below 900 mm.

The pattern shown by HMP and LMP estimates (Table 5, and 7) is essentially the same as for MAP (Fig. 3), with approximately coinciding maxima and minima (even after excluding poorly-sampled bins; Table 7), and little variation. For RT data, HMP values are generally around 140 mm and range from approximately 110 to 160 mm (Table 5). For raw data, the range is similar, and average HMP estimates are only somewhat lower, ~130 mm (Table 5). LMP estimates using RT and raw data are around 40 mm, showing a range of just 2 mm above and below this average (Table 6).

Although estimated paleoprecipitation variables show remarkable stability, some minimal variations are observed (Fig. 3; Table 7): relatively lower values (MAP slightly below 1,000 mm) during the latest Aragonian (11.5–11.2 Ma), and subsequently during the earliest (11.1–10.0 Ma) and latest (9.5–9.0 Ma) Vallesian. However, for the two latter intervals, gaps in the record and a lower sample size may partly account for this decline. Concomitantly, the oldest part of the record (12.5–11.6 Ma) is characterized by slightly higher paleoprecipitation values, with discrete paleoprecipitation maxima at the earliest Vallesian around 11.2–11.1 Ma, and near the early/late Vallesian boundary at 9.9–9.7 Ma (Fig. 3). These Vallesian maxima coincide with exceptionally well sampled bins, which may partly account for this pattern, but this is not the case for the 12.5–11.6 Ma interval.

Paleotemperature estimates and climate classification

Mean annual temperature estimates for the studied interval show even less variability than paleoprecipitation estimates with values generally around 17.0–17.5 °C (Fig. 3; Table 7). Highest values, between 17.5 and 18.0 °C, are recorded during the 12.2–12.0 and the 10.8–10.6 Ma intervals, the latter

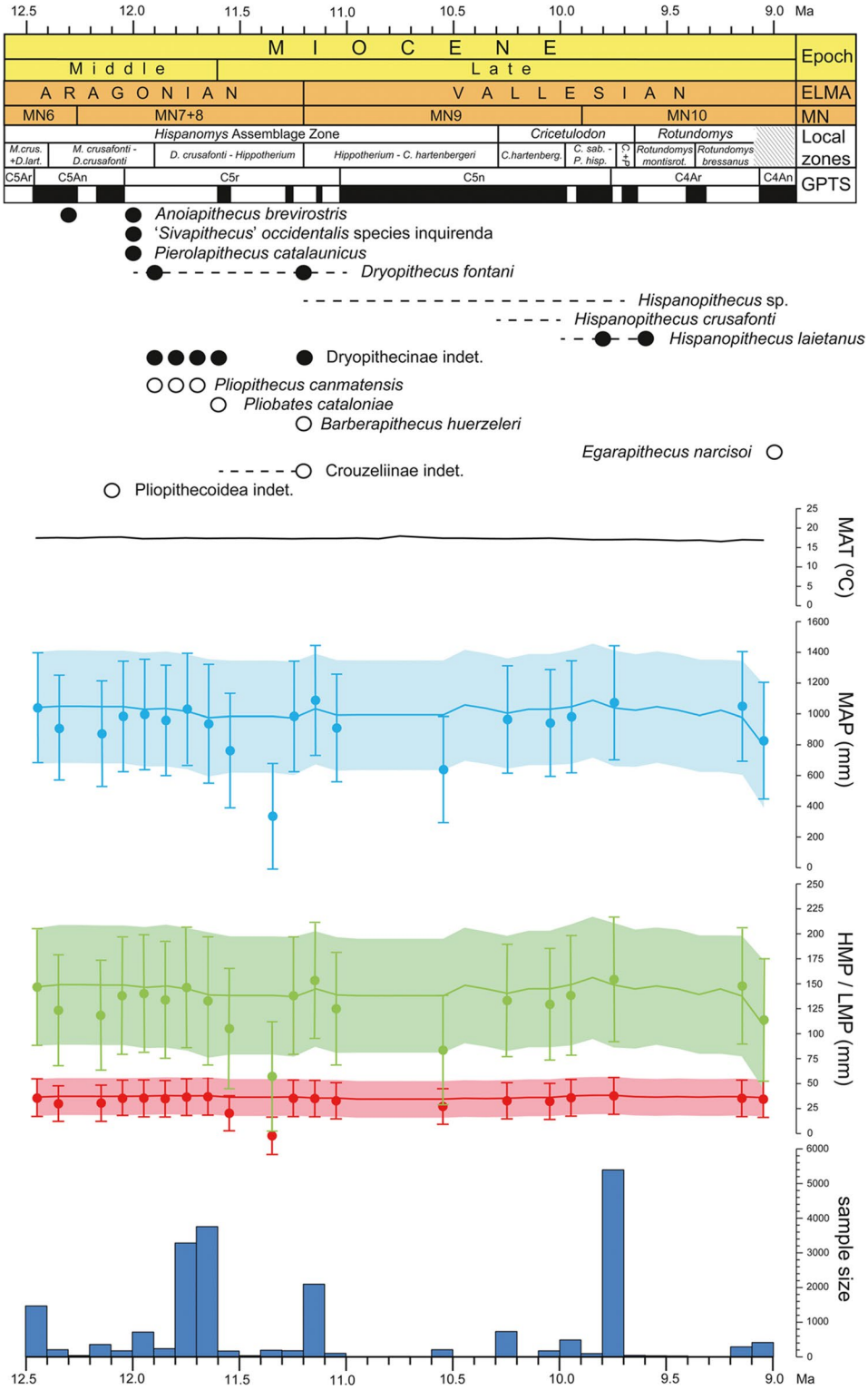

Fig. 3 Primate occurrences, paleotemperature, micromammal-based paleoprecipitation estimates, and micromammal sample size (in number of identified cheek teeth) for the Vallès-Penedès Basin record between 12.5 and 9.0 Ma. Black dots indicate hominoid primates and white dots pliopithecoids. Discontinuous lines indicate dating uncertainty of a few poorly constrained primate occurrences (see Table 1). Mean annual temperature (MAT) is calculated based on calculated global temperature anomalies with respect to current MAT (see text for details). Estimated paleoprecipitation variables comprise mean annual precipitation (MAP), precipitation during the wettest month (HMP, in green) and precipitation during the driest month (LMP, in red). Dots and whiskers represent mean values and 95% confidence intervals calculated using raw data, whereas these parameters are shown as a continuous line and shaded areas for estimates based on a range-through approach (see also Tables 4, 5 and 6). Neogene timescale follows Raffi et al. (2020) while the Vallès-Penedès Basin local biozones are after Casanovas-Vilar et al. (2016a)

coinciding with the brief Tortonian Thermal Maximum (Westerhold et al. 2020). The late Vallesian is characterized by somewhat lower values, which are slightly below 17 °C after 9.5 Ma (Table 7).

Mean annual temperature and rainfall variable estimates are used to assign a Köppen-Geiger climate class (Table 2) to each time bin for both raw and RT data (Table 7). Results generally agree, with a major discrepancy regarding only

Table 4 Mean annual precipitation (MAP, in mm) estimates per time bin based on micromammals. Estimates based on raw data as well as those calculated using a range-through approach are presented for each bin. For each estimate we provide mean values, standard error (SE), and lower and upper 95% confidence intervals (CI)

Bin	Raw data				Range-through approach			
	Mean	SE	Lower CI	Upper CI	Mean	SE	Lower CI	Upper CI
9.1–9.0	819	94	437	1201	789	108	391	1187
9.2–9.1	1044	69	685	1403	971	79	604	1339
9.3–9.2	—	—	—	—	1017	73	622	1345
9.4–9.3	—	—	—	—	984	73	622	1345
9.5–9.4	—	—	—	—	1017	74	655	1380
9.6–9.5	—	—	—	—	1040	69	681	1399
9.7–9.6	—	—	—	—	1017	74	655	1380
9.8–9.7	1068	85	694	1441	1032	85	659	1405
9.9–9.8	—	—	—	—	1082	79	714	1449
10.0–9.9	976	78	609	1343	1040	77	674	1406
10.1–10.0	935	58	585	1285	1024	68	666	1382
10.2–10.1	—	—	—	—	1024	68	666	1382
10.3–10.2	958	60	607	1309	998	65	643	1354
10.4–10.3	—	—	—	—	1029	66	674	1385
10.5–10.4	—	—	—	—	1052	68	694	1410
10.6–10.5	630	55	282	978	987	62	634	1341
10.7–10.6	—	—	—	—	987	62	634	1341
10.8–10.7	—	—	—	—	987	62	634	1341
10.9–10.8	—	—	—	—	987	62	634	1341
11.0–10.9	—	—	—	—	987	62	634	1341
11.1–11.0	902	61	550	1255	986	66	630	1343
11.2–11.1	1083	71	723	1443	1027	66	671	1383
11.3–11.2	978	73	616	1340	968	77	602	1333
11.4–11.3	323	53	−23	670	978	73	616	1340
11.5–11.4	—	—	—	—	978	73	616	1340
11.6–11.5	754	87	379	1129	978	73	616	1340
11.7–11.6	930	100	541	1319	970	90	592	1348
11.8–11.7	1024	78	658	1391	1010	81	640	1379
11.9–11.8	952	72	591	1314	1028	82	658	1398
12.0–11.9	991	73	629	1353	1023	78	657	1390
12.1–12.0	978	73	616	1340	1040	74	677	1404
12.2–12.1	865	52	519	1211	1040	74	677	1404
12.3–12.2	—	—	—	—	1043	74	680	1406
12.4–12.3	899	56	551	1248	1043	74	680	1406
12.5–12.4	1035	70	676	1395	1035	70	676	1395

the 12.4–11.8 Ma interval, for which raw data result in Csa climates and RT data in Cfa. The moderate MAT slightly below 18 °C indicates subtropical climatic conditions (Cxa; Table 2). MAP estimates are moderate to high, being ~1,000 mm for most time bins. They are in the range of present-day temperate humid areas (e.g., central Europe), some subtropical regions (e.g., parts of the eastern and southeastern coasts of Asia and North America), and humid Mediterranean climates (Pfadenhauer and Klötzli 2020). Differences between HMP and LMP, however, indicate moderate rainfall seasonality overall, so that many bins are assigned to subtropical climates with year-round rainfall (Cfa; Table 2), which today occur in the eastern and southeastern humid coasts of Asia. Such conditions were widespread during the earlier part of the studied interval until 11.6 Ma and are later sporadically recorded near the early/late Vallesian boundary (10.0–9.7 Ma) and in the very last interval (9.1–9.0 Ma; Table 7). For all other intervals, a more seasonal Mediterranean climate (Csa; Table 2) is inferred. We must note that the differences in rainfall parameters, which determine the assignment to either Cfa or Csa, are minimal (Table 7), so that small prediction errors could easily shift the inferred climate type. The climate for the studied interval was probably at the boundary between Cfa and Csa, being too humid and poorly seasonal for a typical Mediterranean climate and simultaneously too dry and slightly seasonal for a typical subtropical humid climate.

Table 5 Precipitation during the wettest month (HMP, in mm) estimates per time bin based on micromammals. Estimates based on raw data as well as those calculated using a range-through approach are presented for each bin. For each estimate we provide mean values, standard error (SE), and lower and upper 95% confidence intervals (CI)

Bin	Raw data				Range-through approach			
	Mean	SE	Lower CI	Upper CI	Mean	SE	Lower CI	Upper CI
9.1–9.0	114	16	51	177	110	18	44	175
9.2–9.1	149	12	89	208	138	14	77	200
9.3–9.2	—	—	—	—	145	13	79	200
9.4–9.3	—	—	—	—	140	13	79	200
9.5–9.4	—	—	—	—	145	14	85	206
9.6–9.5	—	—	—	—	148	13	88	208
9.7–9.6	—	—	—	—	145	14	85	206
9.8–9.7	155	17	91	219	149	16	86	213
9.9–9.8	—	—	—	—	157	15	94	219
10.0–9.9	139	14	78	200	150	15	88	211
10.1–10.0	130	10	73	187	145	12	86	205
10.2–10.1	—	—	—	—	145	12	86	205
10.3–10.2	134	10	76	191	141	11	82	200
10.4–10.3	—	—	—	—	145	11	87	204
10.5–10.4	—	—	—	—	149	12	90	208
10.6–10.5	83	8	27	139	139	11	80	197
10.7–10.6	—	—	—	—	139	11	80	197
10.8–10.7	—	—	—	—	139	11	80	197
10.9–10.8	—	—	—	—	139	11	80	197
11.0–10.9	—	—	—	—	139	11	80	197
11.1–11.0	125	10	67	183	139	12	80	198
11.2–11.1	154	12	95	214	145	12	86	204
11.3–11.2	139	13	78	199	137	14	76	199
11.4–11.3	56	8	−1	112	139	13	78	199
11.5–11.4	—	—	—	—	139	13	78	199
11.6–11.5	105	15	43	167	139	13	78	199
11.7–11.6	133	18	67	199	139	17	75	203
11.8–11.7	147	15	85	209	145	15	83	208
11.9–11.8	134	13	74	194	148	16	86	211
12.0–11.9	141	13	80	201	147	15	85	209
12.1–12.0	139	13	78	199	149	14	88	210
12.2–12.1	119	8	62	175	149	14	88	210
12.3–12.2	—	—	—	—	150	14	89	211
12.4–12.3	124	9	67	181	150	14	89	211
12.5–12.4	148	13	88	208	148	13	88	208

Discussion

Sample size effects on paleoprecipitation proxies

Our calculations unambiguously show that, except for a few species, arboreal and invertivorous small mammal taxa were uncommon components of the VP faunas during the studied time interval, so that they will not be recorded if sample size is too small. Casanovas-Vilar et al. (2014) already showed this for the Vallesian small mammal faunas and critically re-evaluated the severity and timing of the Vallesian Crisis, a purportedly 'catastrophic' extinction event occurring at the early/late Vallesian boundary (Agustí and Moyà-Solà 1990; Agustí et al. 1997, 1999, 2003, 2013). Considering that these sampling biases had major effects on calculations of paleobiodiversity dynamics led to the suggestion that the Vallesian Crisis was a more protracted gradual extinction comprising all the late Vallesian and maybe extending into the early Turolian (Casanovas-Vilar et al. 2014, 2016b). Given that CDA uses the relative richness of arboreal and invertivorous taxa (PA, PI) for paleoprecipitation estimates, it would be expected that they are considerably affected by sample size. However, this is only partly true. Even though our statistical tests detect significant positive correlations for MAP, HMP, and LMP with sample size using raw data and not using RT data (Table 3), the estimates using both approaches generally do not differ markedly (Fig. 3; Tables 4–6). Van Dam's (2006) choice for relative rather than

Table 6 Precipitation in the driest month (LMP, in mm) estimates per time bin based on micromammals. Estimates based on raw data as well as those calculated using a range-through approach are presented for each bin. For each estimate we provide mean values, standard error (SE), and lower and upper 95% confidence intervals (CI)

Bin	Raw data				Range-through approach			
	Mean	SE	Lower CI	Upper CI	Mean	SE	Lower CI	Upper CI
9.1–9.0	38	3	20	57	39	3	21	57
9.2–9.1	39	3	21	58	40	3	21	58
9.3–9.2	—	—	—	—	40	3	21	58
9.4–9.3	—	—	—	—	39	3	21	58
9.5–9.4	—	—	—	—	40	3	21	58
9.6–9.5	—	—	—	—	39	3	21	58
9.7–9.6	—	—	—	—	40	3	21	58
9.8–9.7	42	3	23	60	41	3	23	60
9.9–9.8	—	—	—	—	41	3	23	60
10.0–9.9	40	3	21	58	41	3	22	59
10.1–10.0	36	3	18	54	39	3	21	57
10.2–10.1	—	—	—	—	39	3	21	57
10.3–10.2	37	3	19	55	38	3	20	57
10.4–10.3	—	—	—	—	38	3	20	56
10.5–10.4	—	—	—	—	38	3	20	57
10.6–10.5	31	2	13	49	37	3	19	56
10.7–10.6	—	—	—	—	37	3	19	56
10.8–10.7	—	—	—	—	37	3	19	56
10.9–10.8	—	—	—	—	37	3	19	56
11.0–10.9	—	—	—	—	37	3	19	56
11.1–11.0	37	3	19	55	39	3	20	57
11.2–11.1	39	3	21	57	38	3	20	57
11.3–11.2	39	3	21	58	40	3	21	58
11.4–11.3	2	2	−16	20	39	3	21	58
11.5–11.4	—	—	—	—	39	3	21	58
11.6–11.5	24	2	7	42	39	3	21	58
11.7–11.6	41	3	22	59	41	3	22	59
11.8–11.7	41	3	22	59	41	3	22	59
11.9–11.8	39	3	21	57	41	3	22	59
12.0–11.9	40	3	21	58	40	3	22	59
12.1–12.0	39	3	21	58	40	3	22	59
12.2–12.1	35	3	17	53	40	3	22	59
12.3–12.2	—	—	—	—	40	3	22	59
12.4–12.3	34	3	16	52	40	3	22	59
12.5–12.4	40	3	21	58	40	3	21	58

absolute richness numbers was motivated to increase robustness against sample size effects, because it is expected that rare, unrecorded taxa occur across all ecological categories (Online Resource 3: Table S1). Yet, in some cases, insufficient sample size can still result in biased, lower paleoprecipitation estimates, as it happens for the 11.4–11.3 and 10.6–10.5 Ma bins (Fig. 3). Conversely, higher sample sizes may increase these estimates, as it may be the case for the 9.7–9.8 Ma bin (Fig. 3). These patterns are evident using raw data, and still resonate using RT data, although correlations are not significant.

The question of what minimum sample size should be used for CDA is difficult to assess and will not be discussed in detail herein. For some bins with small sample sizes, paleoprecipitation estimates are unrealistically low, whereas for others they are not (Fig. 3). Sample sizes for the mentioned 11.4–11.3 and 10.6–10.5 Ma bins are twice the 100 specimen threshold proposed by Van Dam (2006), so 100 may not be enough for the studied area and time interval. Hardly any differences are observed between paleoprecipitation estimates using raw and RT data when sample size is well above 500 or 1,000 specimens (Fig. 3; Table 7; Online Resource 3: Table S1). Because such a sampling effort has not been applied to most sites and/or time bins, caution is recommended when interpreting smaller samples, at least for the VP. Finally, we must point out that our methods lumped several localities into discrete time bins, whereas CDA was originally designed to work at the locality level.

Table 7 Mean annual temperature (MAT, in °C) based on calculated global temperature anomalies with respect to current MAT, paleoprecipitation estimates (in mm) based on micromammals, and Köppen-Geiger climate classification (see Table 2) for each time bin. For paleoprecipitation estimates only mean values are shown for mean annual precipitation (MAP), wettest month precipitation (HMP) and driest month precipitation (LMP), for confidence intervals and standard errors see Tables 4, 5 and 6. Estimates based on raw data as well as those calculated using a range-through approach are presented for each bin

Bin	Raw data					Range-through approach			
	MAT	MAP	HMP	LMP	climate	MAP	HMP	LMP	climate
9.1–9.0	16.9	819	114	38	Cfa	789	110	39	Cfa
9.2–9.1	17.0	1044	149	39	Csa	971	138	40	Csa
9.3–9.2	16.6	—	—	—	—	1017	145	40	Csa
9.4–9.3	16.9	—	—	—	—	984	140	39	Csa
9.5–9.4	16.8	—	—	—	—	1017	145	40	Csa
9.6–9.5	17.0	—	—	—	—	1040	148	39	Csa
9.7–9.6	17.1	—	—	—	—	1017	145	40	Csa
9.8–9.7	17.0	1068	155	42	Cfa	1032	149	41	Cfa
9.9–9.8	17.0	—	—	—	—	1082	157	41	Cfa
10.0–9.9	17.2	976	139	40	Csa	1040	150	41	Cfa
10.1–10.0	17.4	935	130	36	Csa	1024	145	39	Csa
10.2–10.1	17.3	—	—	—	—	1024	145	39	Csa
10.3–10.2	17.3	958	134	37	Csa	998	141	38	Csa
10.4–10.3	17.3	—	—	—	—	1029	145	38	Csa
10.5–10.4	17.4	—	—	—	—	1052	149	38	Csa
10.6–10.5	17.4	630	83	31	Cfa	987	139	37	Csa
10.7–10.6	17.6	—	—	—	—	987	139	37	Csa
10.8–10.7	17.9	—	—	—	—	987	139	37	Csa
10.9–10.8	17.2	—	—	—	—	987	139	37	Csa
11.0–10.9	17.4	—	—	—	—	987	139	37	Csa
11.1–11.0	17.3	902	125	37	Csa	986	139	39	Csa
11.2–11.1	17.3	1083	154	39	Csa	1027	145	38	Csa
11.3–11.2	17.2	978	139	39	Csa	968	137	40	Csa
11.4–11.3	17.3	323	56	2	B	978	139	39	Csa
11.5–11.4	17.4	—	—	—	—	978	139	39	Csa
11.6–11.5	17.4	754	105	24	Csa	978	139	39	Csa
11.7–11.6	17.3	930	133	41	Cfa	970	139	41	Cfa
11.8–11.7	17.4	1024	147	41	Cfa	1010	145	41	Cfa
11.9–11.8	17.3	952	134	39	Csa	1028	148	41	Cfa
12.0–11.9	17.3	991	141	40	Csa	1023	147	40	Cfa
12.1–12.0	17.7	978	139	39	Csa	1040	149	40	Cfa
12.2–12.1	17.6	865	119	35	Csa	1040	149	40	Cfa
12.3–12.2	17.4	—	—	—	—	1043	150	40	Cfa
12.4–12.3	17.5	899	124	34	Csa	1043	150	40	Cfa
12.5–12.4	17.4	1035	148	40	Csa	1035	148	40	Csa

Therefore, species richness numbers for time bins may mix species that did not actually live together (as they do in the modern calibration set), thus affecting paleoprecipitation estimates. An eventual rigorous assessment of the CDA sample size threshold should consider the locality level and a wide dataset comprising diverse geographic areas.

Inferred climatic values, temporal dynamics, and environments

For the studied interval, estimated MAT ranges between ~16.5–18.0 °C, thus yielding realistic values for this latitude and time, which are further consistent with a subtropical climate (Table 2). Similar values were inferred from Vallesian horse tooth enamel $\delta^{18}O$ for the Spanish inland Teruel Basin, at slightly lower latitudes (Van Dam and Reichart, 2009). In contrast, estimates based on plant leaf physiognomy for the Vallesian of the nearby la Cerdanya Basin, in the Catalan Pyrenees, are lower (~11–14 °C; Tosal et al., 2021; Altolaguirre et al., 2023), but these can be explained by a higher altitude. MAP values are relatively high, generally around 1,000 mm, while HMP and LMP are not particularly high or low and, most importantly, do not show the extreme differences that would indicate a marked rainfall seasonality (Table 7). In a monsoon-influenced climate, HMP would be much higher than LMP, whereas in a typical

Mediterranean one, LMP would reach generally lower values. However, MAP is in the low (or too low) range for typical humid subtropical climates (Cfa; Pfadenhauer and Klötzli 2020) and simultaneously slightly above the range for typical Mediterranean climates (Csa; Pfadenhauer and Klötzli 2020). Not surprisingly, some bins are assigned to Cfa and others to Csa, although they only show minimal variations in paleoprecipitation estimates (Table 7). Perhaps the VP climate during this interval was transitional between Cfa and Csa, with few potential modern analogues, except for the areas where these two classes meet, such as near the northern Adriatic and Black Sea coasts (see updated Köppen-Geiger climate classification maps in Beck et al. 2023). Instead, more typical Cfa and Csa climates might have alternated in the area on a finer temporal scale than the 0.1 Myr level of analysis—so, localities belonging to one or the other would have been mixed when lumping the data into discrete time bins. Nevertheless, we find this second option unlikely because paleoprecipitation estimates for some individual localities, such as Can Poncic 1 and Can Llobateres 1 (CLL1; Van Dam 2006: Table 6), are very similar to those reported for the time bins that include them (10.3–10.2 and 9.8–9. 7 Ma). Furthermore, during most of the Miocene, only the Antarctic ice sheet was present, and it was less extensive than today (Westerhold et al. 2020; Steinthorsdottir et al. 2021). Consequently, first-order astronomical cycles (those with periodicities < 0.1 Myr, such as precession and obliquity), which could have driven Cfa/Csa alternations, likely had a much weaker expression.

Major biomes associated with Csa climates are Mediterranean forest and shrubland, while those occurring at Cfa climates are subtropical evergreen broadleaf and mixed mesophytic forests (Pfadenhauer and Klötzli 2020). The VP landscape during the studied time interval may have been intermediate or may have combined both biomes, with subtropical forests occurring near permanent water masses and at mid altitudes along the reliefs bounding the basin, and dryer landscapes extending into the lowlands.

Interestingly, our results show little variation in the reconstructed climatic variables other than a minimal decrease in MAT during the late Vallesian and marginally higher precipitation during the older part of the record and in a few time bins during the early Vallesian (Fig. 3). This is quite unexpected, as significant faunal turnovers have been reported across the Aragonian/Vallesian transition (Alba et al. 2022a) and, particularly, during the early/late Vallesian boundary, corresponding to the Vallesian Crisis (e.g., Agustí and Moyà-Solà 1990; Agustí et al. 1997, 1999). Such faunal turnovers may have been triggered by small environmental perturbations and/or may have biotic causes. Ongoing research is set to shed light on this issue, which will not be further discussed here.

Comparison with other paleoclimatic proxies

Additional paleoclimatic proxies and paleobotanical data from the VP and adjacent areas can be used to check our interpretations. Small mammals, in particular, have prominently featured in previous studies of the VP late Aragonian and Vallesian paleoenvironments (Casanovas-Vilar and Agustí 2007; Casanovas-Vilar et al. 2008). These have shown that during that time interval the VP micromammal faunas included several insectivorous and other taxa linked to wet forested environments commonly recorded in central European sites, but absent from the inner Iberian basins, which appear to have been noticeably drier. Such a pattern has been studied in greater detail for insectivores at the genus level (Furió et al. 2011). For this group, the VP faunas represent a subset of central European ones, with only a few talpid and dimylid genera missing, while in the inner Iberian ones virtually all the taxa linked to humid forested environments are gone. This biogeographic pattern is also evident from the micromammal-based continental paleoprecipitation estimates based on CDA for the studied time interval (Van Dam 2006: Fig. 9a–c). During MN7+8 (13.8–11.2 Ma in Van Dam 2006), estimated MAP is ~800–1,000 mm for the VP, thus being only slightly lower than for central Europe (~1,000–1,100 mm) and almost twice the estimates for the inner Iberian basins such as Calatayud-Montalbán (~500 mm). The pattern continues into MN9 (11.2–9.7 Ma in Van Dam 2006), but with slightly higher paleoprecipitation values in all three regions, and during MN10 (9.7–8.9 Ma in Van Dam 2006). However, during MN10, MAP decreases markedly in the VP, being just slightly above 700 mm at maximum, close to the highest values recorded for the inner Iberian basins at that time. In general, Van Dam's (2006) paleoprecipitation estimates for the VP agree with our own, although the former were based on very few localities. These estimates, together with faunal similarities between VP and central European faunas, have been taken as strong evidence for the occurrence of similarly forested environments in this coastal basin (Casanovas-Vilar et al. 2005, 2008; Casanovas-Vilar and Agustí 2007). The dryer inner Iberian basins, which lack primates, would belong to a distinct paleobiogeographic province. These studies by Casanovas-Vilar and co-workers revealed a consistent and long-lasting biogeographical pattern, but they did not attempt a detailed reconstruction of the paleoenvironments or climatic variables in the VP. In contrast, other studies have used a range of approaches—including ecometrics (Arranz et al. 2023) and stable isotope analyses (DeMiguel et al. 2021)—to infer climatic variables for selected VP intervals and sites, often with a particular focus on primate occurrences.

Late Aragonian

The late Aragonian part of the ACM sequence has received great attention because of its excellent chronostratigraphic resolution, dense record, and high diversity of hominoid and pliopithecoid primates (Alba et al. 2017, 2022a). Initial studies focused on ACM/BCV1 (12.0 Ma), the type locality of the hominoid *Pierolapithecus catalaunicus* (Moyà-Solà et al. 2004). In addition to a paleobiogeographic analysis of the ACM/BCV1 small mammal assemblage, Casanovas-Vilar et al. (2008) considered the whole ACM fauna known at the time and used the methods developed by Hernández-Fernández (2001) to infer the possible associated biome. These methods use discriminant analysis based on the relative contribution of several selected taxonomic groups to the large mammal sample. Fossil localities are classified based on the discriminant functions according to the composition of several modern localities from different biomes. Results classified ACM as an evergreen tropical rainforest, which is clearly unrealistic, not only considering our paleoprecipitation and paleotemperature estimates but also contemporary paleobotanical data from the region, which indicate subtropical mixed mesophytic forests (Vicente Castells 1988; Sanz de Siria Catalán 1996; Gómez-Gras et al. 2001).

More recently, DeMiguel et al. (2021) used dental microwear coupled with carbon ($\delta^{13}C$) and oxygen ($\delta^{18}O$) stable isotope data of dental enamel of the moschid *Micromeryx*, ubiquitous along the ACM series, to infer MAP and MAT. The analyzed material comes from various ACM sites ranging from 12.38 to 11.60 Ma. $\delta^{18}O$ values were used to infer MAT and yielded surprisingly high estimates, generally above 20 °C for most of the interval, decreasing to ~17 °C only after 11.70 Ma (DeMiguel et al. 2021: Fig. 3). $\delta^{13}C$ values indicated that *Micromeryx* fed exclusively on C_3 vegetation, further yielding very negative values (−26 to −28‰, after conversion to modern dietary equivalents) that would be indicative of a relatively closed canopy. $\delta^{13}C$ values were also used to estimate MAP with the methods of Kohn (2010). Estimated MAP was well above 1,000 mm for the 12.38–11.90 Ma interval, peaking in 1,400 mm near its end, then sharply declined at 11.80 Ma to ~400 mm, to finally rapidly increase again to around 700 mm and keep stable until 11.60 Ma (DeMiguel et al. 2021: Fig. 3). As for the high estimated MAT of DeMiguel et al. (2021), it is mostly consistent with tropical to subtropical climates. However, MAP estimates are low for tropical and subtropical humid forests (Pfadenhauer and Klötzli 2020) and align more with tropical seasonal forests and savannas. Mean annual precipitation estimates based on *Micromeryx* stable isotopes partly agree with our results, which infer MAP values slightly above 1,000 mm for the 12.5–11.7 Ma interval, which mostly includes sites from the ACM sequence (Fig. 3; Table 7). MAP is found to slightly decrease from 11.7 to 11.2 Ma, but not to the level shown by DeMiguel et al. (2021). This is also reflected in the climate classification, since older bins up to 11.6 Ma are assigned to Cfa, whereas younger ones (11.6–11.2 Ma) are classified as Csa (Table 7). The slightly lower MAP, combined with the 3–5 °C lower MAT estimates based on our data, result in different paleoenvironmental reconstructions, closer to subtropical biomes rather than to tropical ones. We consider our MAT estimates more realistic because tropical temperatures are not supported by other proxies, such as contemporary paleobotanical data (Sanz de Siria Catalán 1993).

DeMiguel et al. (2021) further related the apparent rare co-occurrence of hominoid and pliopithecoid primates in the ACM sequence (and elsewhere) to different environmental preferences: the larger-bodied hominoids would have favored denser forested environments, while pliopithecoids would have been able to thrive in more open woodlands. Our results do not support such distinction and show that both hominoids and pliopithecoids tend to be more commonly present at times of minimally higher MAP. However, it is unclear whether this represents a true pattern or has more to do with random chance. Sukselainen et al. (2015) used ecological diversity of associated mammal faunas and dental ecometrics as paleoprecipitation/humidity proxies to study habitat preferences of hominoid and pliopithecoid primates in Eurasia. These authors found that pliopithecoids appear to have been associated with more humid environments than hominoids, which was contradicted by DeMiguel et al. (2021) and is not supported either by our data. Sukselainen et al. (2015) also found that, the few sites where both groups co-occur (such as the early Vallesian sites of Castell de Barberà in the VP or Rudabánya in Hungary), were even more humid. The latter observation is partly supported by our results, since the 11.2–11.1 Ma bin, which would include Castell de Barberà, coincides with one of the paleoprecipitation maxima in the record, both using raw and RT data (Fig. 3; Table 7). Hominoids and pliopithecoids also coincide at the same locality in the ACM series (Alba et al. 2017, 2022a) at 11.9 (ACM/C5-C3) and 11.6 Ma (ACM/C5-D1). Paleoprecipitation estimates for the bins including these localities are not particularly high, further being slightly below average for the 11.6–11.7 Ma bin (Fig. 3; Table 7).

No paleobotanical data are available for the late Aragonian part of the VP record. However, palynological (Gómez-Gras et al. 2001) and macrofloral data (Vicente Castells 1988) from the Montjuïc section, in the nearby Barcelona Basin (Serravallian, 13.6–11.6 Ma) suggest subtropical mixed mesophytic forests, although the presence of leguminous trees in the macroflora (e.g., *Caesalpinia*, *Cassia*, *Gleditschia*, *Robinia*) indicates also some drier woodland

habitats (Sanz de Siria Catalán 1996). Overall, these data are congruent with our MAT and MAP estimates, so that this kind of humid subtropical forests interspersed with drier woodlands may have also defined the zonal vegetation in the VP at that time.

Vallesian

As for Vallesian paleoenvironments, the early late Vallesian (9.76 Ma) locality of CLL1 has deserved the greatest attention, likely because of the recovery of several *Hispanopithecus laietanus* dental remains (Begun et al. 1990; Alba et al. 2012b) and the find of a partial skeleton of the same species in the slightly younger (9.62 Ma) locality of CLL2 within the same section (Moyà-Solà and Köhler 1993, 1996). The CLL section represents a distal inter-channel alluvial plain, with CLL1 corresponding to a poorly drained area with shallow ponds and small lakes (Begun et al. 1990; Marmi et al. 2012; Alba et al. 2012b). Can Llobateres 1 falls in the 9.8–9.7 Ma bin, which stands out as the most densely-sampled bin (Online Resource 3: Table S1) and records a MAP maximum and Cfa climate both using raw and RT data (Table 7). Indeed, the small mammal fauna of the site includes multiple arboreal taxa, including various flying squirrel genera (*Blackia*, *Pliopetaurista*) unknown from other VP sites (Casanovas-Vilar et al. 2015). The mammal fauna is incredibly diverse (~80 species; updated faunal list after Arranz et al. 2023) and many Middle Miocene holdovers (e.g., amphicyonids, barbourofelids, listriodontine suids) are here recorded for the last time in the basin. Besides vertebrates, plant macroremains have also been recovered from various stratigraphic levels at CLL1 (Marmi et al. 2012). The small macrofloral assemblage includes parautochthonous and allochthonous plant remains deposited in marshy areas, with reeds (*Typha*, *Phragmites*), palms (cf. *Sabal* sp.), evergreen laurels (cf. *Cinnamomum* sp.), and abundant fig fruits (*Ficus* sp.), suggesting a dense riparian forest adjacent to a marshy area (Marmi et al. 2012). The absence of deciduous taxa and presence of mega-mesothermal elements indicate a tropical to subtropical climate, although these inferences should be cautiously interpreted given that the plant assemblage corresponds to azonal vegetation—more influenced by local environmental factors than by regional climate. However, such an environment is consistent with the high diversity of arboreal rodents and the presence of suspensory adaptations in *Hispanopithecus* (Moyà-Solà and Köhler 1996; Almécija et al. 2007). On the other hand, abundant semiaquatic beavers (*Chalicomys*, *Euroxenomys*) as well as the presence of the tapirid *Tapirus*, the tragulid *Dorcatherium*, and the bovid *Miotragocerus* support the occurrence of wetlands and permanent water bodies (Arranz et al. 2023; Pandolfi et al. 2025).

Paleoenvironmental inferences drawn on the basis of the composition and structure of the CLL1 macromammal assemblage (Andrews 1996; Hernández Fernández et al. 2003; Costeur 2005; Casanovas-Vilar et al. 2008) consistently identify humid forested environments, but do not agree in assigning the site to subtropical or tropical climates. Recently, Arranz et al. (2023) used the methods of Žliobaitė et al. (2016) to estimate various climatic variables (including MAT, MAP, HMP and LMP; see Arranz et al. 2023: Table 5) from dental ecometrics of the CLL1 herbivorous large mammals. Estimated MAT is 25 °C and that of the coldest month 24 °C, thus effectively situating CLL1 within tropical climates. MAP estimate is 881 mm, ~250 mm lower than ours (Table 7), but HMP attains the surprisingly high value of 2,199 mm and LMP 136 mm, which markedly contrast with our estimates of about 150 and 40 mm, respectively (Table 7). The high precipitation during the driest month is consistent with a rainforest climate (Beck et al. 2023), but the pronounced contrast with the wettest month is more typical of monsoonal regimes. However, a peak monthly precipitation exceeding 2,000 mm would be unrealistically high, as present-day monsoon climates rarely record more than 800–1,000 mm in their wettest month (typically 300–600 mm), even in regions most exposed to the monsoon, such as Bangladesh and northeastern India (Walter 1979; Pfadenhauer and Klötzli 2020). Furthermore, it cannot be that precipitation during a single month (2,199 mm) is higher than MAP (881 mm), so this odd value probably reflects limitations of the method used. Arranz et al. (2023) further inferred the biome of CLL1 using two approaches. The first one just considered estimated MAT and MAP and, using a Whittaker diagram (Whittaker 1971), classified it as a tropical seasonal forest/savanna. Their second approach, using canonical variates analysis of dental ecometric variables of extant sites, identified it as a tropical rainforest, which the authors considered unlikely given associated paleobotanical data. As happened with the ACM sequence, higher MAT estimates result in the assignment of CLL1 to tropical rather than to subtropical climates, although inferred MAP is broadly similar to our results. Considering our inferred MAT and MAP estimates, the 9.8–9.7 Ma bin (Table 7), which includes CLL1, would plot in a Whittaker diagram within the uppermost range of temperate seasonal forests, but very close to the boundary with tropical seasonal forest/savanna.

Since the CLL1 macroflora clearly represents an azonal assemblage, paleobotanical data from other Vallesian sites may provide more clues on dominant biomes. There are few data on early Vallesian vegetation in the VP, but the Tortonian site of Mas Rampinyo (broadly correlated to the early Vallesian) yielded abundant plant macroremains of leguminous trees and shrubs with small xerophilous leaves (*Cassia*,

Leguminosites), plus evergreen laurels (*Cinnamomum*, *Laurus*) and subtropical taxa like soapberries (*Sapindus*; Sanz de Siria Catalán 1993). These are consistent with data from richer early Vallesian macrofloras from the coastal Empordà Basin (about 100 km north of the VP), which suggest a heterogeneous landscape with dense riparian forests and more open woodland or bushland beyond (Tosal et al. 2022). Such environments may have been widespread during the early Vallesian in Catalan coastal basins. Interestingly, sedimentological and faunal data consistently indicate that most other Vallesian hominoid sites in the VP, such as Castell de Barberà (11.2 Ma; Alba et al. 2019) or Can Pallars i Llobateres (10.0–9.7 Ma; Alba et al. 2018), correspond to wetland and riparian environments. These sites have yielded most of the small mammal material for the 11.2–11.1 and 10.0–9.7 intervals, so it is likely that this overrepresentation of wetland environments results in somewhat higher MAP estimates.

Independent paleoenvironmental data for the late Vallesian are extremely scarce. However, a rich and well-preserved flora has been described from Trinxera Sud Autopista 2 (Agustí et al. 2003), a 9.3 Ma locality that is slightly younger than La Tarumba 1 (9.6 Ma), where the last hominoid primates from the VP have been recorded. Geological evidence suggests that Trinxera Sud Autopista 2 also represents a wetland environment, yet its flora differs markedly from that of CLL1. The Trinxera Sud Autopista 2 macroflora points to a mixed mesophytic forest, with nearly half of the arboreal taxa being deciduous (Agustí et al. 2003). Most notably, the mega- mesothermic taxa growing near the water such as palms and fig trees have been replaced by riparian deciduous trees such as alders (*Alnus*), ashes (*Fraxinus*), and poplars (*Populus*). Agustí et al. (2003) compared this association to floras that are found today in parts of central-eastern China, southern Japan, and southeastern North America, where a similar mixture of evergreen broadleaved, warm-temperate and deciduous elements is present (Pfadenhauer and Klötzli 2020). Therefore, they inferred that a similar climate occurred at the VP at the time with MAT of 16–19 °C and MAP above 1,000 mm, which perfectly agrees with our estimates (Table 7). While this flora points to greater temperature seasonality as compared to CLL1, our MAT estimates indicate minimal differences between the bins that would include both sites (Table 7). Our methods are only suitable for estimating MAT at the regional level, so perhaps CLL1 represented a warm microclimate within a generally colder area. Alternative methods, such as stable isotopes, could be used to shed new light on the CLL1 paleoclimate (Arranz et al. 2024). Finally, Agustí et al. (2003) interpreted that temperature seasonality would have increased during the late Vallesian, thus triggering hominoid local extinction. Our results show a very slight MAT decrease of 0.3–0.5 °C from the early to the latest Vallesian, inconsistent with a marked increase in temperature seasonality, which should imply at least a difference of some degrees.

Implications for paleoenvironmental reconstruction of Vallès-Penedès primate habitats

Although they are more common and diverse in tropical forest and woodland environments, primates currently inhabit a broad range of different habitats (Fleagle et al. 2025). Extant (non-human) hominoids, however, generally live in (or near) densely forested equatorial areas in Africa and Southeast Asia (Almécija et al. 2021; Fleagle et al. 2025). However, this does not apply to most of their evolutionary history, as extant hominoids represent a decimated and biased sample of a much larger radiation that had its heyday during the Miocene, when they were found all over the Old World except in its northernmost regions and were represented by multiple species and genera (Almécija et al. 2021; Urciuoli and Alba 2023). Given their wide geographic range, it is almost certain that at least some Miocene hominoids lived in habitats substantially different from those of their extant counterparts. Indeed, various lines of evidence indicate that many Miocene ape-bearing sites correspond to dryer and more seasonal environments (Andrews 2015, 2020). This also appears to have been the case of VP Miocene hominoids. First, our estimated MAT values are in the range of subtropical rather than tropical climates, such as subtropical evergreen broadleaf and mixed mesophytic forests. Second, MAP is also well below the values for tropical rainforests (Af) and monsoon forests (Am), for which it exceeds 2,000 mm/yr (Pfadenhauer and Klötzli 2020). Indeed, MAP is even quite low for a subtropical humid climate (Cfa), at times showing values closer to humid Mediterranean climates (Csa), which would imply the presence of dryer forest and shrubland. Finally, rainfall seasonality does not appear to have been very marked, so VP environments were not as seasonally dry as Mediterranean, monsoon, or savanna climates.

Overall, we can conclude that the VP primates lived in relatively colder and less humid climates than their extant relatives, but that rainfall seasonality was not particularly marked. There is no apparent pattern in primate occurrences (Fig. 3), although hominoids tend to be present and more diverse at times of slightly higher rainfall, which are identified as Cfa climates. On the other hand, we found no significant differences between hominoid and pliopithecoid occurrences, neither evidence that pliopithecoids occurred at significantly drier (contra DeMiguel et al. 2021) or more humid (contra Sukselainen et al. 2015) habitats. Therefore, the occurrence of primates in the VP appears more related to

sampling effort and random chance than to marked environmental differences—even though subtle local paleoenvironmental differences might be at play. On the other hand, the lack of major variations in temperature and paleoprecipitation during the studied time interval questions the hypothesis that Vallesian climatic changes, and concomitant habitat fragmentation determined the local extinction of the group, as previously suggested (Agustí et al. 2003; Marmi et al. 2012). Nevertheless, with the estimated climatic variables showing that the VP climate at the time was at the boundary between Mediterranean (Csa) and humid subtropical (Cfa) climates, it is likely that the environment was not optimal for primates, and these were generally rare and confined to suitable refugia. Perhaps minimal variations in either MAT and/or MAP were enough to trigger their local disappearance, but this hypothesis needs to be critically evaluated, if possible, using other paleoclimatic proxies.

As for specific VP primate habitats, we infer that they mostly inhabited subtropical evergreen broadleaf and mixed mesophytic forests, and maybe ecotones between these forests and more open Mediterranean woodland and shrubland. Currently, this kind of subtropical forests is present in both North America and East Asia, in the cooler part of the subtropical climate area, with a high rainfall (>1,000–1,500 mm) during the growing season (Pfadenhauer and Klötzli 2020). The high diversity of tree species is dominated by deciduous taxa (e.g., alder, beech, hornbeam, deciduous oaks) coexisting with some tropical evergreen species (e.g., cinnamon, laurels, evergreen oaks, and many others). These forests are structurally complex, typically composed of two distinct tree canopies, with deciduous species forming the uppermost layer and evergreen woody taxa restricted to the lower canopy and shrub layer (Pfadenhauer and Klötzli 2020). The Vallès-Penedès primates would have thrived in these habitats, given that they appear to have been strictly arboreal. Partial skeletons of VP hominoids reveal an extant ape-like, orthograde body plan adapted for vertical climbing (Moyà-Solà and Köhler 1996; Moyà-Solà et al. 2004; Susanna et al. 2014) and, in the case of *Hispanopithecus*, even suspensory behaviors (Moyà-Solà and Köhler 1996; Almécija et al. 2007; Alba et al. 2012a)—albeit retaining adaptations for powerful-grasping, above-branch quadrupedalism unlike those of extant apes (Moyà-Solà et al. 2004; Almécija et al. 2007, 2009; Alba et al. 2010a, 2012a). In turn, the forelimb anatomy of the small-bodied pliopithecoid *Pliobates* (Bouchet et al. 2024) suggests a combination of arboreal quadrupedalism and cautious, eclectic climbing, with some degree of suspensory behaviors (Alba et al. 2015; Raventós-Izard et al. 2025). Regarding the diet of VP primates, enamel thickness and microwear analyses indicate that the thick-enameled *Pierolapithecus* was a sclerocarpic (hard-object) frugivore similar to extant *Pongo*, whereas *Anoiapithecus*, *Hispanopithecus*, and the thinner-enameled *Dryopithecus* were soft frugivores (Alba et al. 2010b, 2015; DeMiguel et al. 2014; Fortuny et al. 2021). Pliopithecoids, in turn, would have been mainly frugivorous, with some sclerocarpic component more marked in *Pliopithecus* than in *Pliobates* and *Barberapithecus* (DeMiguel et al. 2013; Alba et al. 2015). In summary, evidence on locomotion and diet of VP hominoids and pliopithecoids is consistent with arboreal habits and feeding variously on ripe or sclerocarpic fruits, depending on the species. Such environments and food resources would have been present in the forested subtropical environments inferred, as well as in the drier ecotones between these forests and more seasonal and open woodlands. Almécija et al. (2021) suggested that specialization for a strictly arboreal life style and a predominantly frugivorous diet may have been key for primate disappearance in Western Europe, as these became a 'specialization trap', and once a particular (and perhaps subtle) environmental threshold was surpassed extinction was inevitable.

Conclusions

The ecological structure of small mammal assemblages from the VP has been used to produce high-resolution paleoprecipitation estimates for the densely sampled 12.5–9.0 Ma interval (late Aragonian–Vallesian). Our approach is based on the relative abundance of arboreal and insectivorous taxa, which are generally rare in the VP record; as a result, sample size moderately influences paleoprecipitation estimates, especially in bins with fewer than 500–1,000 specimens, where rare taxa may be underrepresented. Nevertheless, estimates derived from both raw and RT-corrected data are broadly consistent, supporting the robustness of the method when sampling is adequate.

The results indicate that MAP during the late Aragonian and Vallesian typically hovered around 1,000 mm, with limited rainfall seasonality. Mean annual temperature, inferred through anomalies relative to present values, suggests a subtropical climate (~17–18 °C). Combined, these climatic estimates point to a transitional regime between humid subtropical (Cfa) and Mediterranean (Csa) types. Our paleoprecipitation estimates align with other paleoenvironmental proxies and support the interpretation of the VP as more humid and forested than the inner Iberian basins—where primates are absent—but less so than Central Europe. Such conditions would have supported subtropical evergreen broadleaf and mixed forests interspersed with drier woodland areas, providing suitable (albeit suboptimal) habitats for both hominoid and pliopithecoid primates. We find no

evidence that primate-bearing intervals corresponded to distinctly more forested paleoenvironments, nor clear ecological differences that could explain the presence of pliopithecoids rather than hominoids. While hominoid diversity appears slightly higher during wetter intervals, their presence seems more strongly shaped by sampling intensity and stochastic factors—albeit local paleoenvironmental differences cannot be ruled out.

The reconstructed climates and habitats are consistent with the arboreal locomotor adaptations and dietary preferences of VP primates, although these taxa inhabited climates significantly cooler and less humid than those occupied by their extant relatives. Notably, climatic variables remained relatively stable through time, with only minor variations in MAP and MAT—even across major faunal turnover events such as the Vallesian Crisis at ~9.7 Ma. These results cast doubts on the role of abrupt climatic change in driving local extinctions, including that of hominoids. Their disappearance may instead reflect a more gradual habitat fragmentation extending into the Turolian, or the decline of small, vulnerable populations occupying marginal habitats especially sensitive to subtle climatic perturbations. These alternative scenarios should be further tested using multiple independent paleoenvironmental proxies and performing the analyses for selected localities rather than time bins, while also considering the ecological flexibility and climatic tolerances of Miocene hominoids and pliopithecoids.

Supplementary Information The online version contains supplementary material available at https://doi.org/10.1007/s10914-025-09788-x.

Acknowledgements We are indebted to J. Agustí (ICP) for his valuable comments on the rodent fauna from many sites. We thank M. Misas, S. Arranz and G. Pons-Monjo (ICP) for uploading to the VPDB database many of the raw taxonomic data used in this study. We also thank the countless students and volunteers who devoted many hours to sediment sorting and fossil picking, allowing the recovery of much of the small mammal material. Finally, we thank two anonymous reviewers as well as guest editor J. Arias-Martorell for their comments and corrections, which certainly helped to improve the original manuscript. This work is a tribute to Salvador Moyà-Solà, who often emphasized (even if not always publicly) the need to dedicate time, people and resources to the study of Vallès-Penedès small mammal faunas. Salvador was a tremendous source of inspiration for all of us. To a greater or lesser extent, we owe him much—from research opportunities and fruitful discussions to personal support and guidance. He made a lasting impact not only on mammalian paleontology but also on us personally, and we consider it an honor to call Salva our friend. For the first author (I.C.-V.), this impact was especially profound, and a separate acknowledgement is warranted. Thank you Salva, for everything you have done for me: for giving me some of the first opportunities to pursue a career in mammalian paleontology, and for inviting me to contribute to some of the most remarkable discoveries in Catalan paleontology. You have always supported and encouraged me, even during my lowest moments, and I deeply apologize if I did not always deliver. I can say, without hesitation, that I am the paleontologist—and the person—I am today in great part thanks to you. So once again, thank you, Salva, for everything.

Author contributions The basic design of the study was set out by I.C.-V. and J.V.D. All authors compiled the raw taxonomic data. I.C.-V. carried the calculations and analyses except for the paleoprecipitation estimates, which were carried out by I.C.-V. and J.V.D. The text was primarily written by I.C.-V. with contributions from all other authors.

Funding Open Access funding provided thanks to the CRUE-CSIC agreement with Springer Nature. Open Access funding provided by CERCA through the CRUE-CSIC agreement with Springer Nature. This work is part of R+D+I projects PID2020-117289GBI00/MCIN/AEI/10.13039/501100011033/ and PID2024-159434NB-I00/MCIN/AEI/10.13039/501100011033/, funded by the Agencia Estatal de Investigación of the Spanish Ministry of Science and Innovation. Research has also been supported by the Generalitat de Catalunya/CERCA Programme and the Agència de Gestió d'Ajuts Universitaris i de Recerca of the Generalitat de Catalunya (Consolidated Research Group 2022 SGR 00620).

Data availability All data associated with this study are provided in the published article and associated supplementary files. Virtually all the studied fossils are housed and adequately curated at the ICP (Sabadell, Spain), being accessible to other researchers.

Declarations

Competing interests The authors declare no competing interests.

References

Agustí J, Moyà-Solà S (1990) Mammal extinctions in the Vallesian (Upper Miocene). In: Kauffman EG, Walliser OH (eds) Extinction Events in Earth History. Springer Verlag, Berlin, pp 425–432. https://doi.org/10.1007/BFb0011163

Agustí J, Cabrera L, Moyà-Solà S (1985) Sinopsis estratigráfica del Neógeno de la fosa del Vallés-Penedés. Paleontol Evol 18:57–81

Agustí J, Köhler M, Moyà-Solà S, Cabrera L, Garcés M, Parés JM (1996) Can Llobateres: the pattern and timing of the Vallesian hominoid radiation reconsidered. J Hum Evol 31:143–155. https://doi.org/10.1006/jhev.1996.0055

Agustí J, Cabrera L, Garcés M, Parés JM (1997) The Vallesian mammal succession in the Vallès-Penedès basin (northeast Spain): Paleomagnetic calibration and correlation with global events. Palaeogeogr Palaeoclimatol Palaeoecol 133:149–180. https://doi.org/10.1016/S0031-0182(97)00084-9

Agustí J, Cabrera L, Garcés M, Llenas M (1999) Mammal turnover and global climate change in the late Miocene terrestrial record of the Vallès-Penedès Basin (NE Spain). In: Agustí J, Rook L, Andrews P (eds) Hominoid Evolution and Climatic Change in

Europe: Volume 1: The Evolution of Neogene Terrestrial Ecosystems in Europe. Cambridge University Press, Cambridge, pp 397–412. https://doi.org/10.1017/CBO9780511542329.020

Agustí J, Sanz de Siria A, Garcés M (2003) Explaining the end of the hominoid experiment in Europe. J Hum Evol 45:145–153. https://doi.org/10.1016/S0047-2484(03)00091-5

Agustí J, Cabrera L, Garcés M (2013) The Vallesian Mammal Turnover: A Late Miocene record of decoupled land-ocean evolution. Geobios 42:151–157. https://doi.org/10.1016/j.geobios.2012.10.005

Alba DM (2012) Fossil apes from the Vallès-Penedès Basin. Evol Anthropol 21:254–269. https://doi.org/10.1002/evan.21312

Alba DM (2025) Research trajectory, works, and legacy of Salvador Moyà-Solà as a vertebrate paleobiologist. J Mamm Evol 32:24. https://doi.org/10.1007/s10914-025-09760-9

Alba DM, Casanovas-Vilar I (2022) Prologue: From Crusafont to NOW. Paleontol Evol Mem Espec 9:7–12

Alba DM, Moyà-Solà S (2012a) On the identity of a hominoid male upper canine from the Vallès-Penedès Basin figured by Pickford (2012). Estud Geol 68:149–153. https://doi.org/10.3989/egeol.40900.180

Alba DM, Moyà-Solà S (2012b). A new pliopithecid genus (Primates: Pliopithecoidea) from Castell de Barberà (Vallès-Penedès Basin, Catalonia, Spain). Am J Phys Anthropol 147:88–112. https://doi.org/10.1002/ajpa.21630

Alba DM, Moyà-Solà S, Casanovas-Vilar I, Galindo J, Robles JM, Rotgers C, Furió M, Angelone C, Köhler M, Garcés M, Cabrera L, Almécija S, Obradó P (2006) Los vertebrados fósiles del Abocador de Can Mata (els Hostalets de Pierola, l'Anoia, Cataluña), una sucesión de localidades del Aragoniense superior (MN6 y MN7+8) de la cuenca del Vallès-Penedès. Campañas 2002–2003, 2004 y 2005. Estud Geol 62:295–312. https://doi.org/10.3989/egeol.0662127

Alba DM, Almécija S, Moyà-Solà, S. (2010a). Locomotor inferences in *Pierolapithecus* and *Hispanopithecus*: Reply to Deane and Begun (2008). *J Hum Evol 59* :143–149. https://doi.org/10.1016/j.jhevol.2010.02.002

Alba DM, Fortuny J, Moyà-Solà S (2010b) Enamel thickness in the Middle Miocene great apes *Anoiapithecus*, *Pierolapithecus* and *Dryopithecus*. Proc R Soc Lond B 277:2237–2245. https://doi.org/10.1098/rspb.2010.0218

Alba DM, Moyà-Solà S, Malgosa A, Casanovas-Vilar I, Robles JM, Almécija S, Galindo J, Rotgers C, Mengual JVB (2010c) A new species of *Pliopithecus* Gervais, 1849 (Primates: Pliopithecidae) from the Middle Miocene (MN8) of Abocador de Can Mata (els Hostalets de Pierola, Catalonia, Spain). Am J Phys Anthropol 141:52–75. https://doi.org/10.1002/ajpa.21114

Alba DM, Moyà-Solà S, Almécija S (2011) A partial hominoid humerus from the middle Miocene of Castell de Barberà (Vallès-Penedès Basin, Catalonia, Spain). Am J Phys Anthropol 144:365–381. https://doi.org/10.1002/ajpa.21417

Alba DM, Almécija S, Casanovas-Vilar I, Méndez JM, Moyà-Solà S (2012a) A partial skeleton of *Hispanopithecus laietanus* from Can Feu and the mosaic evolution of crown-hominoid positional behaviors. PLoS One 7:e39617. https://doi.org/10.1371/journal.pone.0039617

Alba DM, Casanovas-Vilar I, Almécija S, Robles JM, Arias-Martorell J, Moyà-Solà S (2012b) New dental remains of *Hispanopithecus laietanus* (Primates: Hominidae) from Can Llobateres 1 and the taxonomy of Late Miocene hominoids from the Vallès-Penedès Basin (NE Iberian Peninsula). J Hum Evol 63:231–246. https://doi.org/10.1016/j.jhevol.2012.05.009

Alba DM, Moyà-Solà S, Robles JM, Galindo J (2012c) Brief Communication: The oldest pliopithecid record in the Iberian Peninsula based on new material from the Vallès-Penedès Basin. Am J Phys Anthropol 147:135–140. https://doi.org/10.1002/ajpa.21631

Alba DM, Fortuny J, Pérez de los Ríos M, Zanolli C, Almécija S, Casanovas-Vilar I, Robles JM, Moyà-Solà S (2013) New dental remains of *Anoiapithecus* and the first appearance datum of hominoids in the Iberian Peninsula. J Hum Evol 65:573–584. https://doi.org/10.1016/j.jhevol.2013.07.003

Alba DM, Almecija S, DeMiguel D, Fortuny J, de los Rios MP, Pina M, Robles JM, Moyà-Solà S (2015) Miocene small-bodied ape from Eurasia sheds light on hominoid evolution. Science 350:aab2625. https://doi.org/10.1126/science.aab2625

Alba DM, Casanovas-Vilar I, Garcés M, Robles JM (2017) Ten years in the dump: An updated review of the Miocene primate-bearing localities from Abocador de Can Mata (NE Iberian Peninsula). J Hum Evol 102:12–20. https://doi.org/10.1016/j.jhevol.2016.09.012

Alba DM, Casanovas-Vilar I, Furió M, García-Paredes I, Angelone C, Jovells-Vaqué S, Luján ÀH, Almécija S, Moyà-Solà S (2018) Can Pallars i Llobateres: A new hominoid-bearing locality from the late Miocene of the Vallès-Penedès Basin (NE Iberian Peninsula). J Hum Evol 121:254–259

Alba DM, Garcés M, Casanovas-Vilar I, Robles JM, Pina M, Moyà-Solà S, Almécija S (2019) Bio- and magnetostratigraphic correlation of the Miocene primate-bearing site of Castell de Barberà to the earliest Vallesian. J Hum Evol 132:32–46. https://doi.org/10.1016/j.jhevol.2019.04.006

Alba DM, Fortuny J, Robles JM, Bernardini F, Pérez de los Ríos M, Tuniz C, Moyà-Solà S, Zanolli C (2020) A new dryopithecine mandibular fragment from the middle Miocene of Abocador de Can Mata and the taxonomic status of '*Sivapithecus*' *occidentalis* from Can Vila (Vallès-Penedès Basin, NE Iberian Peninsula). J Hum Evol 145:102790. https://doi.org/10.1016/j.jhevol.2020.102790

Alba DM, Robles JM, Casanovas-Vilar I, Beamud E, Bernor RL, Cirilli O, DeMiguel D, Galindo J, Llopart I, Pons-Monjo G, Sánchez IM, Vinuesa V, Garcés M (2022a) A revised (earliest Vallesian) age for the hominoid-bearing locality of Can Mata 1 based on new magnetostratigraphic and biostratigraphic data from Abocador de Can Mata (Vallès-Penedès Basin, NE Iberian Peninsula). J Hum Evol 170:103237. https://doi.org/10.1016/j.jhevol.2022.103237

Alba DM, Torres J, DeMiguel D, Casanovas-Vilar I (2022b) The "Vallès-Penedès Miocene Vertebrates" paleobiodiversity database. Paleontol Evolució Mem Espec 9:59–60

Alba DM, Bouchet F, Fortuny J, Robles JM, Galindo J, Luján ÀH, Moyà-Solà S, Zanolli C (2024a) New remains of the Miocene great ape *Anoiapithecus brevirostris* from Abocador de Can Mata. J Hum Evol 188:103497. https://doi.org/10.1016/j.jhevol.2024.103497

Alba DM, Siarabi S, Arranz SG, Galindo J, McKenzie S, Vinuesa V, Robles JM, Casanovas-Vilar I (2024b) New suid remains from the early Vallesian (Late Miocene) site of Can Missert (Vallès-Penedès Basin). J Mamm Evol 31:19. https://doi.org/10.1007/s10914-024-09712-9

Alba DM, Siarabi S, Arranz SG, McKenzie S, Casanovas-Vilar I (2025) Dental remains of '*Parachleuastochoerus*' *valentini* (Suidae: Tetraconodontinae) from the early Late Miocene of Sant Quirze (Vallès-Penedès Basin, NE Iberian Peninsula): Taxonomic and phylogenetic implications. Swiss J Palaeontol 144:9. https://doi.org/10.1186/s13358-024-00344-3

Almécija S, Alba DM, Moyà-Solà S, Köhler M (2007) Orang-like manual adaptations in the fossil hominoid *Hispanopithecus laietanus*: first steps towards great ape suspensory behaviours. Proc R Soc B 274:2375–2384. https://doi.org/10.1098/rspb.2007.0750

Almécija S, Alba DM, Moyà-Solà S (2009) *Pierolapithecus* and the functional morphology of Miocene ape hand phalanges: paleobiological and evolutionary implications. J Hum Evol 57:284–297. https://doi.org/10.1016/j.jhevol.2009.02.008

Almécija S, Alba DM, Moyà-Solà S (2012) The thumb of Miocene apes: new insights from Castell de Barberà (Catalonia, Spain). Am J Phys Anthropol 148:436–450. https://doi.org/10.1002/ajpa.22071

Almécija S, Hammond AS, Thompson NE, Pugh KD, Moyà-Solà S, Alba DM (2021) Fossil apes and human evolution. Science 372 :eabb4363. https://doi.org/10.1126/science.abb4363

Altolaguirre Y, Postigo-Mijarra JM, Casas-Gallego M, Moreno-Domínguez R, Barrón E (2023) Mapping the Late Miocene Pyrenean forests of the La Cerdanya Basin, Spain. Forests 14:1471. https://doi.org/10.3390/f14071471

Andrews P (1996) Palaeoecology and hominoid palaeoenvironments. Biol Rev 71:257–300. https://doi.org/10.1111/j.1469-185X.1996.tb00749.x

Andrews P (2015) An Ape's View of Human Evolution, 1st ed. Cambridge University Press, Cambridge. https://doi.org/10.1017/CBO9781316180938

Andrews P (2020) Last common ancestor of apes and humans: Morphology and environment. Folia Primatol 91:122–148. https://doi.org/10.1159/000501557

Arranz SG, Casanovas-Vilar I, Žliobaitė I, Abella J, Angelone C, Azanza B, Bernor R, Cirilli O, DeMiguel D, Furió M, Pandolfi L, Robles JM, Sánchez IM, van den Hoek Ostende LW, Alba DM (2023) Paleoenvironmental inferences on the Late Miocene hominoid-bearing site of Can Llobateres (NE Iberian Peninsula): An ecometric approach based on functional dental traits. J Hum Evol 185:103441. https://doi.org/10.1016/j.jhevol.2023.103441

Arranz SG, Misas-Alcántara M, Comes P, Kimura Y, Villanueva J, Flynn LJ, Alba DM, Casanovas-Vilar I (2024) Paleoenvironmental reconstruction of the Late Miocene primate-bearing site of Can Llobateres (NE Iberian Peninsula) based on carbon and oxygen stable isotopes from herbivorous mammal teeth. J Vertebr Paleontol Program and Abstracts 2024:210.

Badgley C, Finarelli JA (2013) Diversity dynamics of mammals in relation to tectonic and climatic history: comparison of three Neogene records from North America. Paleobiology 39:373–399. https://doi.org/10.1666/12024

Badgley C, Morgan ME, Pilbeam D (eds) (2025) At the Foot of the Himalayas. Paleontology and Ecosystem Dynamics of the Siwalik Record. Johns Hopkins University Press, Baltimore. https://doi.org/10.56021/9781421450278

Barry JC, Morgan ME, Flynn LJ, Pilbeam D, Behrensmeyer AK, Raza SM, Khan IA, Badgley C, Hicks J, Kelley J (2002) Faunal and environmental change in the late Miocene Siwaliks of northern Pakistan. Paleobiology 28(S2):1–71. https://doi.org/10.1666/0094-8373(2002)28[1:FAECIT]2.0.CO;2

Bartrina MT, Cabrera L, Jurado MJ, Guimerà J, Roca E (1992) Evolution of the central Catalan margin of the Valencia trough (western Mediterranean). Tectonophysics 203:219–247. https://doi.org/10.1016/0040-1951(92)90225-U

Beck HE, McVicar TR, Vergopolan N, Berg A, Lutsko NJ, Dufour A, Zeng Z, Jiang X, van Dijk AIJM, Miralles DG (2023) High-resolution (1 km) Köppen-Geiger maps for 1901–2099 based on constrained CMIP6 projections. Sci Data 10:724. https://doi.org/10.1038/s41597-023-02549-6

Begun DR (1992) *Dryopithecus crusafonti* sp. nov., a new Miocene hominoid species from Can Ponsic (Northeastern Spain). Am J Phys Anthropol 87:291–309. https://doi.org/10.1002/ajpa.1330870306

Begun DR, Moyà-Solà S, Köhler M (1990) New Miocene hominoid specimens from Can Llobateres (Vallès Penedès, Spain) and their geological and paleoecological context. J Hum Evol 19:255–268

Bouchet F, Zanolli C, Urciuoli A, Almécija S, Fortuny J, Robles JM, Beaudet A, Moyà-Solà S, Alba DM (2024) The Miocene primate *Pliobates* is a pliopithecoid. Nat Commun 15:2822. https://doi.org/10.1038/s41467-024-47034-9

Bouchet F, Zanolli C, Fortuny J, Moyà-Solà S, Alba DM (2025). Further insight into an unnamed, medium-sized crouzeliid pliopithecoid from the Vallès-Penedès Basin (NE Iberian Peninsula). Swiss J Palaeontol 144:58. https://doi.org/10.1186/s13358-025-00404-2

Cabrera L, Calvet F (1996) Onshore Neogene record in NE Spain: Vallès-Penedès and El Camp half-grabens (NW Mediterranean). In: Friend PF, Dabrio CJ (eds) Tertiary Basins of Spain: Record of Crustal Kinematics. Cambridge University Press, Cambridge, pp 97–105. https://doi.org/10.1017/CBO9780511524851.017

Cabrera L, Calvet F, Guimerà J, Permanyer A (1991) El registro sedimentario miocénico en los semigrabens del Vallès-Penedès y de el Camp: Organización secuencial y relaciones tectónica sedimentación. In: Colombo F (ed), I Congreso del Grupo Español del Terciario. Libro-Guía Excursión nº 4. Vic

Cabrera L, Roca E, Garcés M, de Porta J (2004) Estratigrafía y evolución tectonosedimentaria oligocena superior-neógena del sector central del margen catalán (Cadena Costero-Catalana). In: Vera JA (ed) Geología de España. Sociedad Geológica de España and Instituto Geológico y Minero de España, Madrid, pp 569–573

Cabrera Pérez L (1979) Estudio estratigráfico y sedimentológico de los depósitos continentales basales de la depresión del Vallès-Penedès. Bachelor dissertation, Universitat de Barcelona

Casanovas-Vilar I, Agustí J (2007) Ecogeographical stability and climate forcing in the Late Miocene (Vallesian) rodent record of Spain. Palaeogeogr Palaeoclimatol Palaeoecol 248:169–189. https://doi.org/10.1016/j.palaeo.2006.12.002

Casanovas-Vilar I, Moyà-Solà S, Agustí J, Köhler M (2005) The geography of a faunal turnover: Tracking the Vallesian Crisis. In: Elewa AMT (ed) Migration of Organisms. Springer, Berlin, pp 247–300. https://doi.org/10.1007/3-540-26604-6_9

Casanovas-Vilar I, Alba DM, Moyà-Solà S, Galindo J, Cabrera L, Garcés M, Furió M, Robles JM, Köhler M, Angelone C (2008) Biochronological, taphonomical, and paleoenvironmental background of the fossil great ape *Pierolapithecus catalaunicus* (Primates, Hominidae). J Hum Evol 55:589–603. https://doi.org/10.1016/j.jhevol.2008.05.004

Casanovas-Vilar I, García-Paredes I, Alba DM, Van den Hoek Ostende LW, Moyà-Solà S (2010) The European Far West: Miocene mammal isolation, diversity and turnover in the Iberian Peninsula. J Biogeogr 37:1079–1093. https://doi.org/10.1111/j.1365-2699.2010.02286.x

Casanovas-Vilar I, Van den Hoek Ostende LW, Furió M, Madern PA (2014) The range and extent of the Vallesian Crisis (Late Miocene): new prospects based on the micromammal record from the Vallès-Penedès basin (Catalonia, Spain). J Iber Geol 40:29–48. https://doi.org/10.5209/rev_JIGE.2014.v40.n1.44086

Casanovas-Vilar I, Almécija S, Alba DM (2015) Late Miocene flying squirrels from Can Llobateres 1 (Vallès-Penedès Basin, Catalonia): systematics and palaeobiogeography. Palaeobiodivers Palaeoenviron 95:353–372. https://doi.org/10.1007/s12549-015-0192-1

Casanovas-Vilar I, Garcés M, Van Dam J, García-Paredes I, Robles JM, Alba DM (2016a) An updated biostratigraphy for the late Aragonian and Vallesian of the Vallès-Penedès Basin (Catalonia). Geol Acta 14:195–217. https://doi.org/10.1344/GeologicaActa2016.14.3.1

Casanovas-Vilar I, Madern A, Alba DM, Cabrera L, García-Paredes I, van den Hoek Ostende LW, DeMiguel D, Robles JM, Furió M, van Dam J, Garcés M, Angelone C, Moyà-Solà S (2016b) The Miocene mammal record of the Vallès-Penedès Basin (Catalonia). C R Palevol 15:791–812. https://doi.org/10.1016/j.crpv.2015.07.004

Casanovas-Vilar I, Torres J, DeMiguel D, Alba DM (2018) Introducing: the Vallès-Penedès Miocene Vertebrates Paleobiodiversity Database. In: The Role of NOW in the Future of the Past.

Abstract Book. NOW Meeting in Bratislava , 9–10 October 2018. Bratislava, pp 1–2

Casanovas-Vilar I, Jovells-Vaqué S, DeMiguel D, Madurell-Malapeira J, Furió M, Van Den Hoek Ostende LW, Luján ÀH, Sanisidro Ó, García-Paredes I, Robles JM, Cabrera Pérez L, Garcés M, Alba DM (2021) El Miocè inferior de la conca del Vallès-Penedès: un registre excepcional dels canvis climàtics i faunístics. Trib Arqueol 2018–2019:139–171

Casanovas-Vilar I, Garcés M, Marcuello Á, Abella J, Madurell-Malapeira J, Jovells-Vaqué S, Cabrera L, Galindo J, Beamud E, Ledo JJ, Queralt P, Martí A, Sanjuan J, Martín-Closas C, Jiménez-Moreno G, Luján ÀH, Villa A, DeMiguel D, Sánchez IM, Robles JM, Furió M, Ostende LWV den H, Sánchez-Marco A, Sanisidro Ó, Valenciano A, García-Paredes I, Angelone C, Pons-Monjo G, Azanza B, Delfino M, Bolet A, Grau-Camats M, Vizcaíno-Varo V, Mormeneo D, Kimura Y, Moyà-Solà S, Alba DM (2022a) Els Casots (Subirats, Catalonia), a key site for the Miocene vertebrate record of Southwestern Europe. Hist Biol 34:1494–1508. https://doi.org/10.1080/08912963.2022.2043296

Casanovas-Vilar I, Jovells-Vaqué S, Alba DM (2022b) The Miocene high-resolution record of the Vallès-Penedès Basin (Catalonia). Paleontol Evol Mem Espec 9:79–122

Chevalier M, Davis BAS, Heiri O, Seppä H, Chase BM, Gajewski K, Lacourse T, Telford RJ, Finsinger W, Guiot J, Kühl N, Maezumi SY, Tipton JR, Carter VA, Brussel T, Phelps LN, Dawson A, Zanon M, Vallé F, Nolan C, Mauri A, de Vernal A, Izumi K, Holmström L, Marsicek J, Goring S, Sommer PS, Chaput M, Kupriyanov D (2020) Pollen-based climate reconstruction techniques for late Quaternary studies. Earth Sci Rev 210:103384. https://doi.org/10.1016/j.earscirev.2020.103384

Costeur L (2005) Cenogram analysis of the Rudabánya mammalian community: palaeoenvironmental interpretations. Palaeontogr Ital 303–307

Crusafont i Sabater M (2019) Miquel Crusafont i l'Origen de l'Home. Comanegra, Barcelona

Crusafont Pairó M (1950) La cuestión del llamado Meótico español. Arrahona 1950(1–2):41–48

Crusafont Pairó M, Truyols Santonja J (1960) Sobre la caracterización del Vallesiense. Not Com Inst Geol Min Esp 60:109–126

DeMiguel D, Alba DM, Moyà-Solà S (2013). European pliopithecid diets revised in the light of dental microwear in *Barberapithecus huerzeleri* and *Pliopithecus canmatensis*. Am J Phys Anthropol 151:573–582. https://doi.org/10.1002/ajpa.22299

DeMiguel D, Alba DM, Moyà-Solà S (2014) Dietary specialization during the evolution of Western Eurasian hominoids and the extinction of European great apes. PLoS One 9:e97442. https://doi.org/10.1371/journal.pone.0097442

DeMiguel D, Domingo L, Sánchez IM, Casanovas-Vilar I, Robles JM, Alba DM (2021) Palaeoecological differences underlie rare co-occurrence of Miocene European primates. BMC Biol 19:6. https://doi.org/10.1186/s12915-020-00939-5

Domingo MS, Badgley C, Azanza B, DeMiguel D, Alberdi MT (2014) Diversification of mammals from the Miocene of Spain. Paleobiology 40:196–220. https://doi.org/10.1666/13043

Fleagle JG, Baden AL, Gilbert CC (2025) Primate Adaptation and Evolution, 4th ed. Academic Press, London. https://doi.org/10.1016/C2017-0-03837-5

Flynn LJ, Pilbeam D, Barry JC, Morgan ME, Raza SM (2016) Siwalik synopsis: A long stratigraphic sequence for the Later Cenozoic of South Asia. C R Palevol 15:877–887. https://doi.org/10.1016/j.crpv.2015.09.015

Foote M (2000) Origination and extinction components of taxonomic diversity: general problems. Paleobiology 26(sp4):74–102. https://doi.org/10.1666/0094-8373(2000)26[74:OAECOT]2.0.CO;2

Fortuny J, Zanolli C, Bernardini F, Tuniz C, Alba DM (2021) Dryopithecine palaeobiodiversity in the Iberian Miocene revisited on the basis of molar endostructural morphology. Palaeontology 64:531–554. https://doi.org/10.1111/pala.12540

Furió M, Casanovas-Vilar I, van den Hoek Ostende LW (2011) Predictable structure of Miocene insectivore (Lipotyphla) faunas in Western Europe along a latitudinal gradient. Palaeogeogr Palaeoclimatol Palaeoecol 304:219–229. https://doi.org/10.1016/j.palaeo.2010.01.039

Garcés M, Agustí J, Cabrera L, Parés JM (1996) Magnetostratigraphy of the Vallesian (late Miocene) in the Vallès-Penedès Basin (northeast Spain). Earth Planet Sci Lett 142:381–396. https://doi.org/10.1016/0012-821X(96)00110-0

Garcés Crespo M (1995) Magnetoestratigrafía de las sucesiones del Mioceno medio y superior del Vallès Occidental (Depresión del Vallès-Penedès, N.E. de España): Implicaciones biocronológicas y cronoestratigráficas. Doctoral dissertation, Universitat de Barcelona

García-Paredes I, Álvarez-Sierra MÁ, Van den Hoek Ostende LW, Hernández Ballarín V, Hordijk K, López Guerrero P, Oliver A, Peláez-Campomanes P (2016). The Aragonian and Vallesian high-resolution micromammal succession in the Calatayud-Montalbán Basin (Aragón, Spain). C R Palevol 15:781–789. https://doi.org/10.1016/j.crpv.2015.09.014

Golpe Posse JM (1993) Los Hispanopitecos (Primates, Pongidae) de los yacimientos del Vallès-Penedès (Cataluña, España). II: Descripción del material existente en el Instituto de Paleontología de Sabadell. Paleontol Evol 26–27:151–224

Gómez-Gras D, Parcerisa D, Calvet F, Porta F, Solé de Porta N, Civís J (2001) Stratigraphy and petrology of the Miocene Montjuïc delta (Barcelona, Spain). Acta Geol Hisp 36:115–136

Hammer Ø, Harper D. A. T. (2024). *Paleontological Data Analysis*, *2nd ed.* John Wiley & Sons, Hoboken. https://doi.org/10.1002/9781119933960

Hansen J, Sato M, Russell G, Kharecha P (2013) Climate sensitivity, sea level and atmospheric carbon dioxide. Philos Trans R Soc 371:20120294 https://doi.org/10.1098/rsta.2012.0294

Harrison T, Van der Made J, Ribot F (2002) A new middle Miocene pliopithecid from Sant Quirze, northern Spain. J Hum Evol 42:371–377. https://doi.org/10.1006/jhev.2001.0551

Hernández Fernández M, Salesa MJ, Sánchez IM, Morales J (2003) Paleoecología del género *Anchitherium* von Meyer, 1834 (Equidae, Perissodactyla, Mammalia) en España: Evidencias a partir de las faunas de macromamíferos. Col Paleontol Vol Extr 1:253–280

Hernández-Fernández M (2001) Bioclimatic discriminant capacity of terrestrial mammal faunas. Glob Ecol Biogeogr 10:189–204. https://doi.org/10.1046/j.1466-822x.2001.00218.x

Hilgen FJ, Lourens LJ, Van Dam JA (2012) The Neogene Period. In: Gradstein FM, Ogg JG, Schmitz M, Ogg G (eds) The Geologic Time Scale 2012. Elsevier, Amsterdam, pp 923–978. https://doi.org/10.1016/B978-0-444-59425-9.00029-9

IIBM Corp. (2022). IBM SPSS Statistics for Windows, Version 29.0. Armonk, NY: IBM Corp

Jovells-Vaqué S, Casanovas-Vilar I (2021) Dispersal and early evolution of the first modern cricetid rodents in Western Europe: new data from the Vallès-Penedès Basin (Catalonia). C R Palevol 20:401–439. https://doi.org/10.5852/cr-palevol2021v20a22

Kay RF, Madden RH (1997) Mammals and rainfall: paleoecology of the middle Miocene at La Venta (Colombia, South America). J Hum Evol 32:161–199. https://doi.org/10.1006/jhev.1996.0104

Kohn MJ (2010) Carbon isotope compositions of terrestrial C3 plants as indicators of (paleo)ecology and (paleo)climate. Proc Natl Acad Sci USA 107:19691–19695. https://doi.org/10.1073/pnas.1004933107

Legendre S, Montuire S, Maridet O, Escarguel G (2005) Rodents and climate: A new model for estimating past temperatures. Earth Planet Sci Lett 235:408–420. https://doi.org/10.1016/j.epsl.2005.04.018

Marmi J, Casanovas-Vilar I, Robles JM, Moyà-Solà S, Alba DM (2012) The paleoenvironment of *Hispanopithecus laietanus* as revealed by paleobotanical evidence from the Late Miocene of Can Llobateres 1 (Catalonia, Spain). J Hum Evol 62:412–423. https://doi.org/10.1016/j.jhevol.2011.12.003

McGarigal K, Cushman S, Stafford S (2000) Multivariate Statistics for Wildlife and Ecology Research. Springer, New York

Mein P (1975) Résultats du groupe de travail des vertébrés. In: Sénes J (ed) Report on Activity of RCMNS Working Groups (1971–1975). 6. Congress of the Regional Committee of Mediterranean Neogene Stratigraphy, Proceedings. International Union of Geological Sciences, Committee on Mediterranean Neogene Stratigraphy, Bratislava, pp 78–81

Mein P (1999) European Miocene mammal biochronology. In: Rössner GE, Heissig K (eds) The Miocene Land Mammals of Europe. Verlag Dr. Friedrich Pfeil, Munich, pp 25–38

Montuire S, Maridet O, Legendre S (2006) Late Miocene–Early Pliocene temperature estimates in Europe using rodents. Palaeogeogr Palaeoclimatol Palaeoecol 238:247–262. https://doi.org/10.1016/j.palaeo.2006.03.026

Moyà-Solà S, Agustí J (1990) Bioevents and mammal successions in the Spanish Miocene. In: Lindsay EH, Fahlbusch V, Mein P (eds) European Neogene Mammal Chronology. Plenum Press, New York, pp 357–373. https://doi.org/10.1007/978-1-4899-2513-8_21

Moyà-Solà S, Köhler M (1993) Recent discoveries of *Dryopithecus* shed new light on evolution of great apes. Nature 365:543–545. https://doi.org/10.1038/365543a0

Moyà-Solà S, Köhler M (1996) A *Dryopithecus* skeleton and the origins of great-ape locomotion. Nature 379:156–159. https://doi.org/10.1038/379156a0

Moyà-Solà S, Köhler M, Alba DM (2001) *Egarapithecus narcisoi*, a new genus of Pliopithecidae (Primates, Catarrhini) from the Late Miocene of Spain. Am J Phys Anthropol 114:312–324. https://doi.org/10.1002/ajpa.1043

Moyà-Solà S, Köhler M, Alba DM, Casanovas-Vilar I, Galindo J (2004) *Pierolapithecus catalaunicus*, a new middle Miocene great ape from Spain. Science 306:1339–1344. https://doi.org/10.1126/science.1103094

Moyà-Solà S, Alba DM, Almécija S, Casanovas-Vilar I, Köhler M, DeEsteban-Trivigno S, Robles JM, Galindo J, Fortuny J (2009a) A unique Middle Miocene European hominoid and the origins of the great ape and human clade. Proc Natl Acad Sci USA 106:9601–9606. https://doi.org/10.1073/pnas.0811730106

Moyà-Solà S, Köhler M, Alba DM, Casanovas-Vilar I, Galindo J, Robles JM, Cabrera L, Garcés M, Almécija S, Beamud E (2009b) First partial face and upper dentition of the middle Miocene hominoid *Dryopithecus fontani* from Abocador de Can Mata (Vallès-Penedès Basin, Catalonia, NE Spain): taxonomic and phylogenetic implications. Am J Phys Anthropol 139:126–145. https://doi.org/10.1002/ajpa.20891

Ogg JG (2020) Geomagnetic Polarity Time Scale. In: Gradstein FM, Ogg JG, Schmitz MD, Ogg GM (eds) Geologic Time Scale 2020. Elsevier, Amsterdam, pp 159–192. https://doi.org/10.1016/B978-0-12-824360-2.00005-X

Pandolfi L, Arranz SG, Almécija S, Galindo J, Luján ÀH, Pina M, Urciuoli A, Casanovas-Vilar I, Alba DM (2025) Late Miocene Tapiridae from Vallès-Penedès Basin (NE Iberian Peninsula): Taxonomic and paleoenvironmental Implications. Swiss J Palaeontol 144:3. https://doi.org/10.1186/s13358-024-00342-5

Peel MC, Finlayson BL, McMahon TA (2007) Updated world map of the Köppen-Geiger climate classification. Hydrol Earth Syst Sci 11:1633–1644. https://doi.org/10.5194/hess-11-1633-2007

Pfadenhauer JS, Klötzli FA (2020) Global Vegetation: Fundamentals, Ecology and Distribution. Springer, Cham. https://doi.org/10.1007/978-3-030-49860-3

Puth M-T, Neuhäuser M, Ruxton GD (2015) Effective use of Spearman's and Kendall's correlation coefficients for association between two measured traits. Anim Behav 102:77–84. https://doi.org/10.1016/j.anbehav.2015.01.010

R Core Team (2025) R: A language and environment for statistical computing. R Foundation for Statistical Computing, Vienna. https://www.R-project.org/

Raffi I, Wade BS, Pälike H, Beu AG, Cooper R, Crundwell MP, Krijgsman W, Moore T, Raine I, Sardella R, Vernyhorova YV (2020) The Neogene period. In: Gradstein FM, Ogg JG, Schmitz MD, Ogg GM (eds) Geologic Time Scale 2020. Elsevier, Amsterdam, pp 1141–1215. https://doi.org/10.1016/B978-0-12-824360-2.00029-2

Raventós-Izard G, Monclús-Gonzalo O, Moyà-Solà S, Alba DM, Arias-Martorell J (2025) Ulnar morphology of *Pliobates cataloniae* (Pliopithecoidea: Crouzeliidae): Insights into catarrhine locomotor diversity and forelimb evolution. J Hum Evol 202:103663. https://doi.org/10.1016/j.jhevol.2025.103663

Reumer JWF (1995) The effect of paleoclimate on the evolution of the Soricidae (Mammalia, Insectivora). In: Vrba E, Denton GH, Partridge TC, Burckle LH (eds) Paleoclimate and Evolution, with Emphasis on Human Origins. Yale University Press, New Haven, pp 135–147

Roca E, Guimerà J (1992) The Neogene structure of the eastern Iberian margin: Structural constraints on the crustal evolution of the Valencia trough (western Mediterranean). Tectonophysics 203:203–218. https://doi.org/10.1016/0040-1951(92)90224-T

Roca E, Sans M, Cabrera L, Marzo M (1999) Oligocene to Middle Miocene evolution of the central Catalan margin (northwestern Mediterranean). Tectonophysics 315:209–229. https://doi.org/10.1016/S0040-1951(99)00289-9

Sanz de Siria Catalán A (1993) Datos sobre la paleoclimatología y paleoecología del Neógeno del Vallès-Penedès según las macrofloras halladas en la cuenca y zonas próximas. Paleontol Evol 26–27:281–289

Sanz de Siria Catalán A (1996) La evolución de las paleofloras en las cuencas cenozoicas catalanas. Acta Geol Hisp 29:169–189

Servei Meteorològic de Catalunya (2008) Atles Climàtic de Catalunya 1961–1990. Servei Meteorològic de Catalunya, Institut Cartogràfic de Catalunya, and Universitat de Barcelona, Barcelona

Steinthorsdottir M, Coxall HK, Boer AM de, Huber M, Barbolini N, Bradshaw CD, Burls NJ, Feakins SJ, Gasson E, Henderiks J, Holbourn AE, Kiel S, Kohn MJ, Knorr G, Kürschner WM, Lear CH, Liebrand D, Lunt DJ, Mörs T, Pearson PN, Pound MJ, Stoll H, Strömberg C a. E (2021) The Miocene: the future of the past. Paleoceanogr Paleoclimatol 36:e2020PA004037. https://doi.org/10.1029/2020PA004037

Sukselainen L, Fortelius M, Harrison T (2015) Co-occurrence of pliopithecoid and hominoid primates in the fossil record: An ecometric analysis. J Hum Evol 84:25–41. https://doi.org/10.1016/j.jhevol.2015.04.009

Susanna I, Alba DM, Almécija S, Moyà-Solà S (2014) The vertebral remains of the late Miocene great ape *Hispanopithecus laietanus* from Can Llobateres 2 (Vallès-Penedès Basin, NE Iberian Peninsula). J Hum Evol 73:15–34. https://doi.org/10.1016/j.jhevol.2014.05.009

Tosal A, Verduzco O, Martín-Closas C (2021) CLAMP-based palaeoclimatic analysis of the late Miocene (Tortonian) flora from La Cerdanya Basin of Catalonia, Spain, and an estimation of the palaeoaltitude of the eastern Pyrenees. Palaeogeogr Palaeoclimatol Palaeoecol 564:110186. https://doi.org/10.1016/j.palaeo.2020.110186

Tosal A, Coward SR, Casanovas-Vilar I, Martín-Closas C (2022) Palaeoenvironmental reconstruction of the late Miocene macroflora of La Bisbal d'Empordà (Catalonia, Spain). Comparison with small mammals. Rev Palaeobot Palynol 297:104583. https://doi.org/10.1016/j.revpalbo.2021.104583

Trewartha GT, Horn LH (1980) An Introduction to Climate, 5th ed. McGraw-Hill, New York

Truyols i Santonja J (1986) L'obra científica del doctor Miquel Crusafont i Pairó (1910–1983). Butll Inst Cat Hist Nat 53:19–36

Uhen MD, Barnosky AD, Bills B, Blois J, Carrano MT, Carrasco MA, Erickson GM, Eronen JT, Fortelius M, Graham RW, Grimm EC, O'Leary MA, Mast A, Piel WH, Polly PD, Säilä LK (2013) From card catalogs to computers: databases in vertebrate paleontology. J Vertebr Paleontol 33:13–28. https://doi.org/10.1080/02724634.2012.716114

Urciuoli A, Alba DM (2023) Systematics of Miocene apes: State of the art of a neverending controversy. J Hum Evol 175:103309. https://doi.org/10.1016/j.jhevol.2022.103309

Van Dam JA (2006) Geographic and temporal patterns in the late Neogene (12–3 Ma) aridification of Europe. The use of small mammals as paleoprecipitation proxies. Paleogeogr Paleoclimatol Paleoecol 238:190–218. https://doi.org/10.1016/j.palaeo.2006.03.025

Van Dam JA, Reichart GJ (2009) Oxygen and carbon isotope signatures in late Neogene horse teeth from Spain and application as temperature and seasonality proxies. Paleogeogr Paleoclimatol Paleoecol 274:64–81. https://doi.org/10.1016/j.palaeo.2008.12.022

Van Dam JA, Utescher T (2016) Plant- and micromammal-based paleoprecipitation proxies: Comparing results of the Coexistence and Climate-Diversity Approach. Palaeogeogr Palaeoclimatol Palaeoecol 443:18–33. https://doi.org/10.1016/j.palaeo.2015.11.010

Van Dam JA, Alcalá L, Alonso Zarza A, Calvo JP, Garcés M, Krijgsman W (2001) The upper Miocene mammal record from the Teruel-Alfambra region (Spain). The MN system and continental stage/age concepts discussed. J Vertebr Paleontol 21:367–385. https://doi.org/10.1671/0272-4634(2001)021[0367:TUMMRF]2.0.CO;2

Van Dam JA, Abdul Aziz H, Ángeles Álvarez Sierra M, Hilgen FJ, van den Hoek Ostende LW, Lourens LJ, Mein P, van der Meulen AJ, Pelaez-Campomanes P (2006) Long-period astronomical forcing of mammal turnover. Nature 443:687–691. https://doi.org/10.1038/nature05163

Van Dam JA, Krijgsman W, Abels HA, García-Paredes I, López Guerrero P, Peláez-Campomanes P, Ventra D (2014) Updated chronology for Middle to Late Miocene mammal sites of the Daroca area (Calatayud-Montalbán Basin, Spain). Geobios 47:325–334. https://doi.org/10.1016/j.geobios.2014.07.002

Van Dam JA, Mein P, Garcés M, Van Balen RT, Furió M, Alcalá L (2023) Macroevolutionary and macroecological response of Iberian rodents to late Neogene climatic oscillations and events. Glob Planet Change 227:104153. https://doi.org/10.1016/j.gloplacha.2023.104153

Van der Made J, Ribot F (1999) Additional hominoid material from the Miocene of Spain and remarks on hominoid dispersals into Europe. Contrib Tert Quat Geol 36:25–39

Van der Meulen AJ, García-Paredes I, Álvarez-Sierra MA, Van den HoekOstende LW, Hordijk K, Oliver A, Peláez-Campomanes P (2012). Updated Aragonian biostratigraphy: small mammal distribution and its implications for the Miocene European Chronology. Geol Acta 10:159–179. https://doi.org/10.1344/105.000001710

Vicente Castells J (1988) La Flora Fòssil de Montjuïc (Barcelona). Centre d'Estudis de la Natura del Barcelonès-Nord, Santa Coloma de Gramanet

Villalta Comella JF de, Crusafont Pairó M (1941) Hallazgo del "Dryopithecus fontani", Lartet, en el Vindoboniense de la cuenca Vallés-Penedés. Bol Inst Geol Min Esp 55:131–142

Walter H (1979) Vegetation of the Earth and Ecological Systems of the Geobiosphere. Springer-Verlag, New York. https://doi.org/10.1007/978-1-4684-0468-5

Westerhold T, Marwan N, Drury AJ, Liebrand D, Agnini C, Anagnostou E, Barnet JSK, Bohaty SM, Vleeschouwer DD, Florindo F, Frederichs T, Hodell DA, Holbourn AE, Kroon D, Lauretano V, Littler K, Lourens LJ, Lyle M, Pälike H, Röhl U, Tian J, Wilkens RH, Wilson PA, Zachos JC (2020) An astronomically dated record of Earth's climate and its predictability over the last 66 million years. Science 369:1383–1387. https://doi.org/10.1126/science.aba6853

Whittaker RH (1971) Communities and Ecosystems. MacMillan, New York

Žliobaitė I, Rinne J, Tóth AB, Mechenich M, Liu L, Behrensmeyer AK, Fortelius M (2016) Herbivore teeth predict climatic limits in Kenyan ecosystems. Proc Natl Acad Sci USA 113:12751–12756. https://doi.org/10.1073/pnas.1609409113